

Dina Johar PhD thesis - Physiology and Pathophysiology
List of images

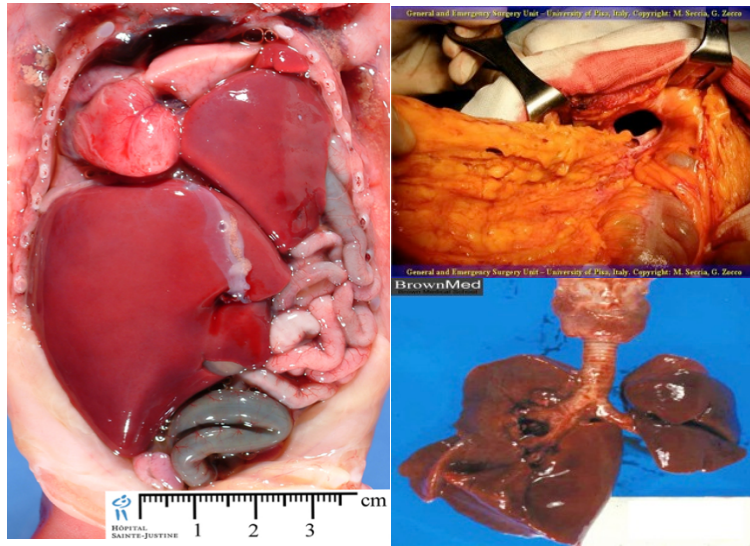
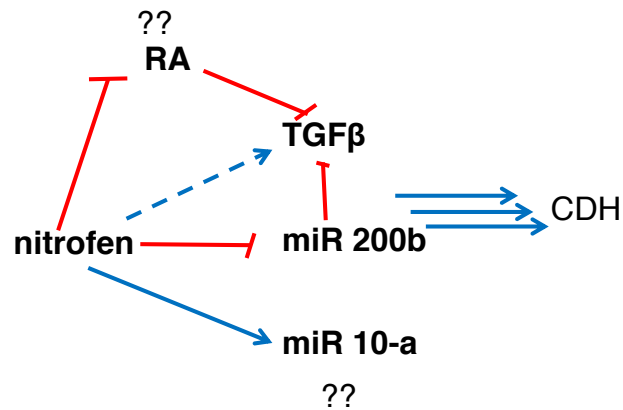


Figure 1.1. Human CDH showing lung hypoplasia and herniation of the GI organs into the chest cavity, and surgical closure of the diaphragmatic hole, unilateral hypoplasia. Photo at the lower right from (18). Photos at the upper right and left are available online from <https://www.slideshare.net/FTmed38/topic-cdh> as of April 18, 2018.



Nitrofen → ~~RARE~~ LacZ → blue

Nitrofen → miR10a LacZ → blue

Nitrofen → ~~SMAD~~ Luc → luminescence

Figure 1.2. Transforming growth factor β (TGF β) is targeted by miR 200 b. Using a heat map, Keijzer and Puri (14) performed a microarray screen with 317 microRNAs comparing human control and CDH lungs. They observed higher levels of miR 200b and miR 10-a in human hypoplastic CDH lungs compared to age-matched controls and that was controversial to the scenario that occurs in rats when the expression was reduced early throughout development and then increased towards term. Nitrofen-induced miR-200b inhibition was associated with reduced airway branching morphogenesis. Eventually, this led to our thinking about exploring what nitrofen does to the transcriptome as primary to further explore its mechanism. Nitrofen promotes TGF β signaling and it does this through abolishing miR 200 b expression. Others observed that RA regulates miR 10-a expression and is important to CDH progression. It also blocks TGF β . In using RARELacZ, every cell that responds to RA is blue. Therefore, if RA miR 200 b LacZ is blocked, every cell that responds to miR 200 b is blue. Upon blockage of RA SMADLuc, every cell that responds to TGF β is luminescent. Consequently, if these promoters are suppressed it becomes possible to see the total effect on the expression and function of miR 10-a or 200 b, which could be informative of their role throughout development.

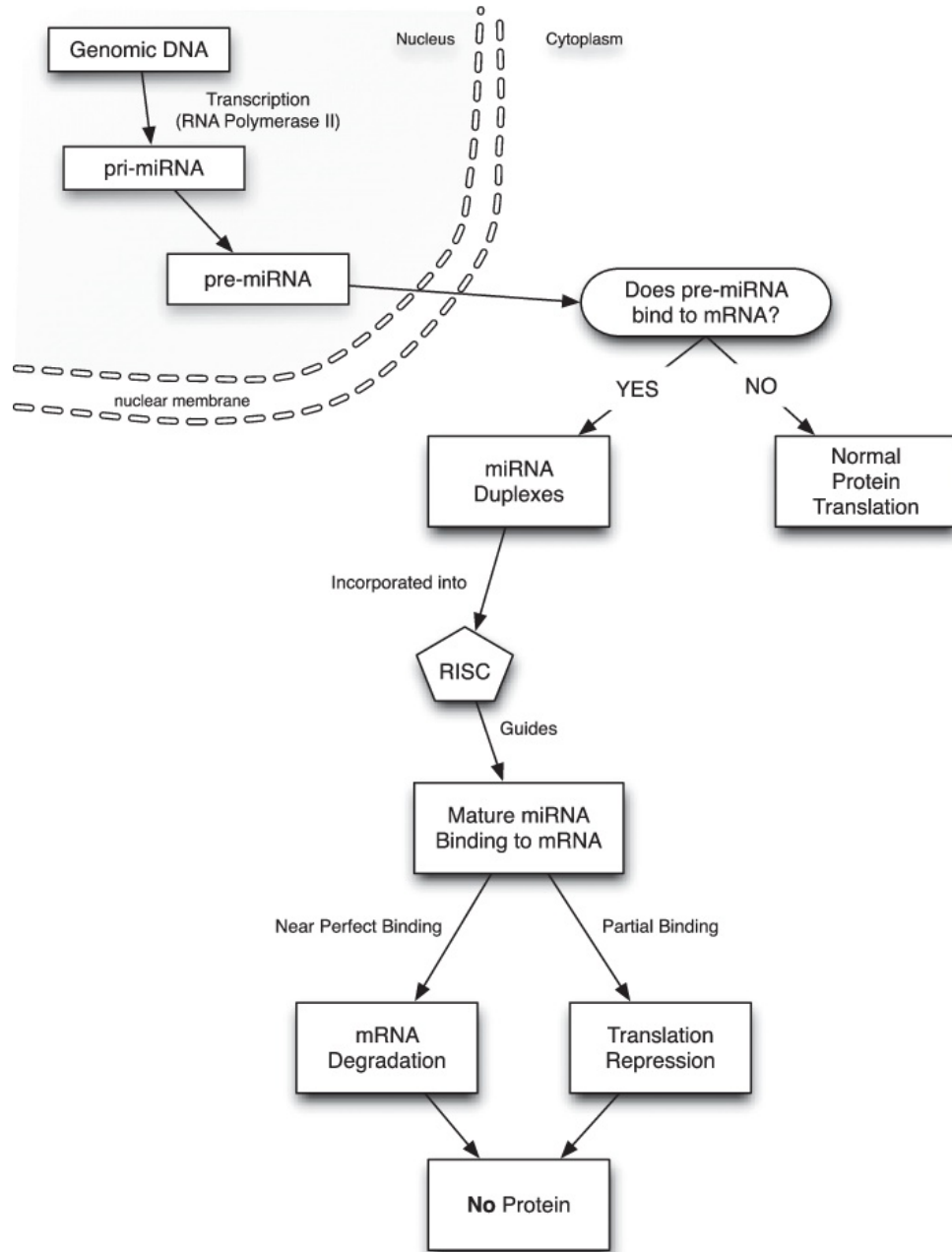


Figure 2.1. A schematic overview of miRNA biogenesis pathways. Shown are two pathways for miRNA function: degradation of mRNA and normal mRNA functions ([185](#)).

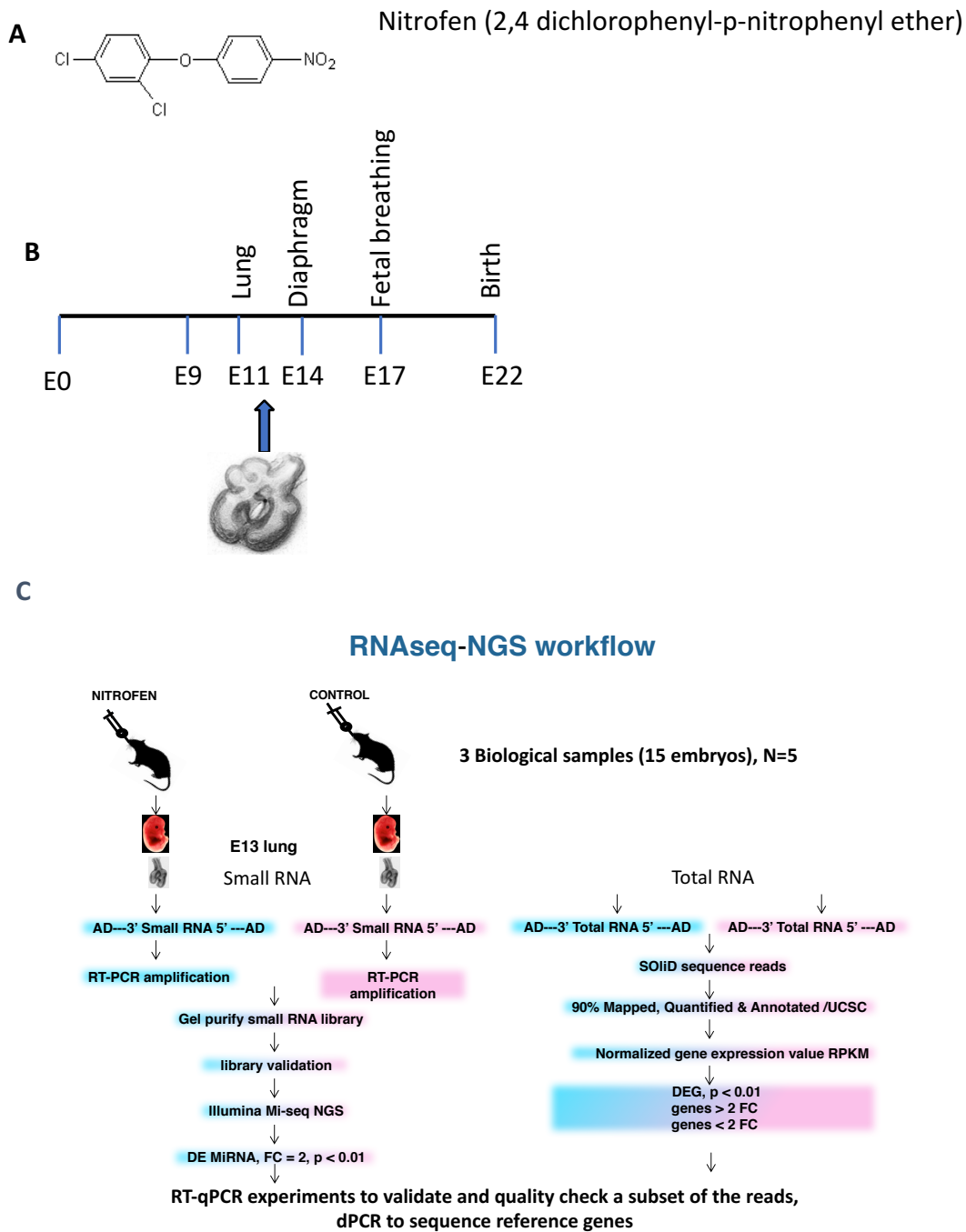


Figure 3.1. The nitrofen rat model. A. The chemical structure of nitrofen. B. E13 lung provides the phenotype characteristics of 80% CDH and 100% pulmonary hypoplasia (PH). C. RNAseq-NGS workflow. N= number, AD= Adaptor, DEG= Differentially expressed genes, FC=Fold Change, UCSC= The University of California Santa Cruz-annotated refGenes, RPKM= Kilobase Per Million Reads.

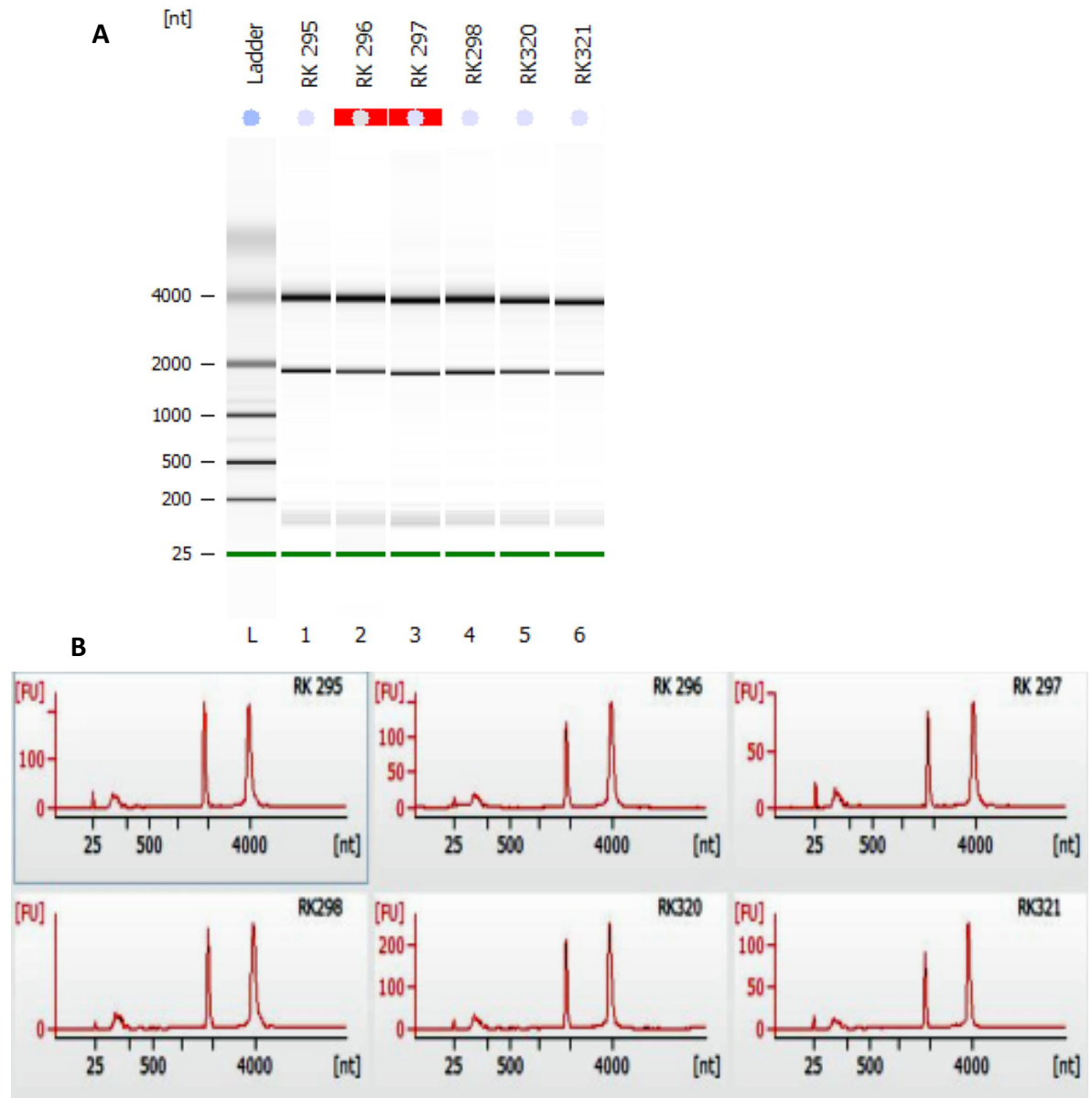


Figure 3.2. RNA quality check of pooled total RNA extracts in triplicate samples of nitrofen treated and control E13.5 embryos before sequencing. A) Capillary based gel electrophoresis and B) electrophoretogram using a BioAnalyzer 2100 (Agilent), version 2.6, sensitivity in picograms.

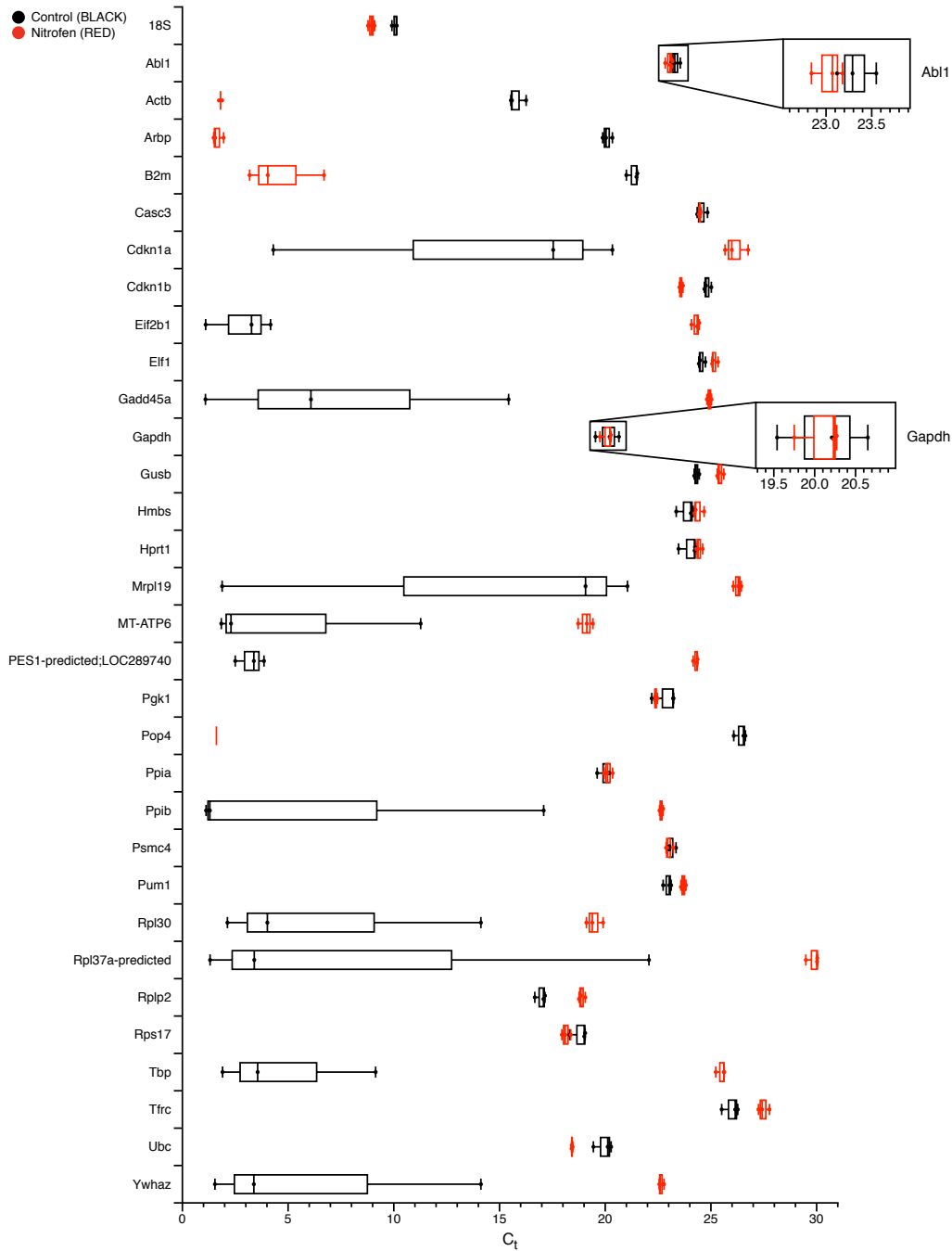


Figure 3.3. TaqMan Assay Validation. Endogenous genes tested (y-axis) were compared to their Ct (x-axis). Box plots show distribution of true biological replicates at E21 from nitrofen and control treated rat lungs. Best candidates, ABLT1 and GAPDH, were selected based upon coefficient of variance and m-fold calculations. CV: 0.0769, M-value: 0.2221. (191).

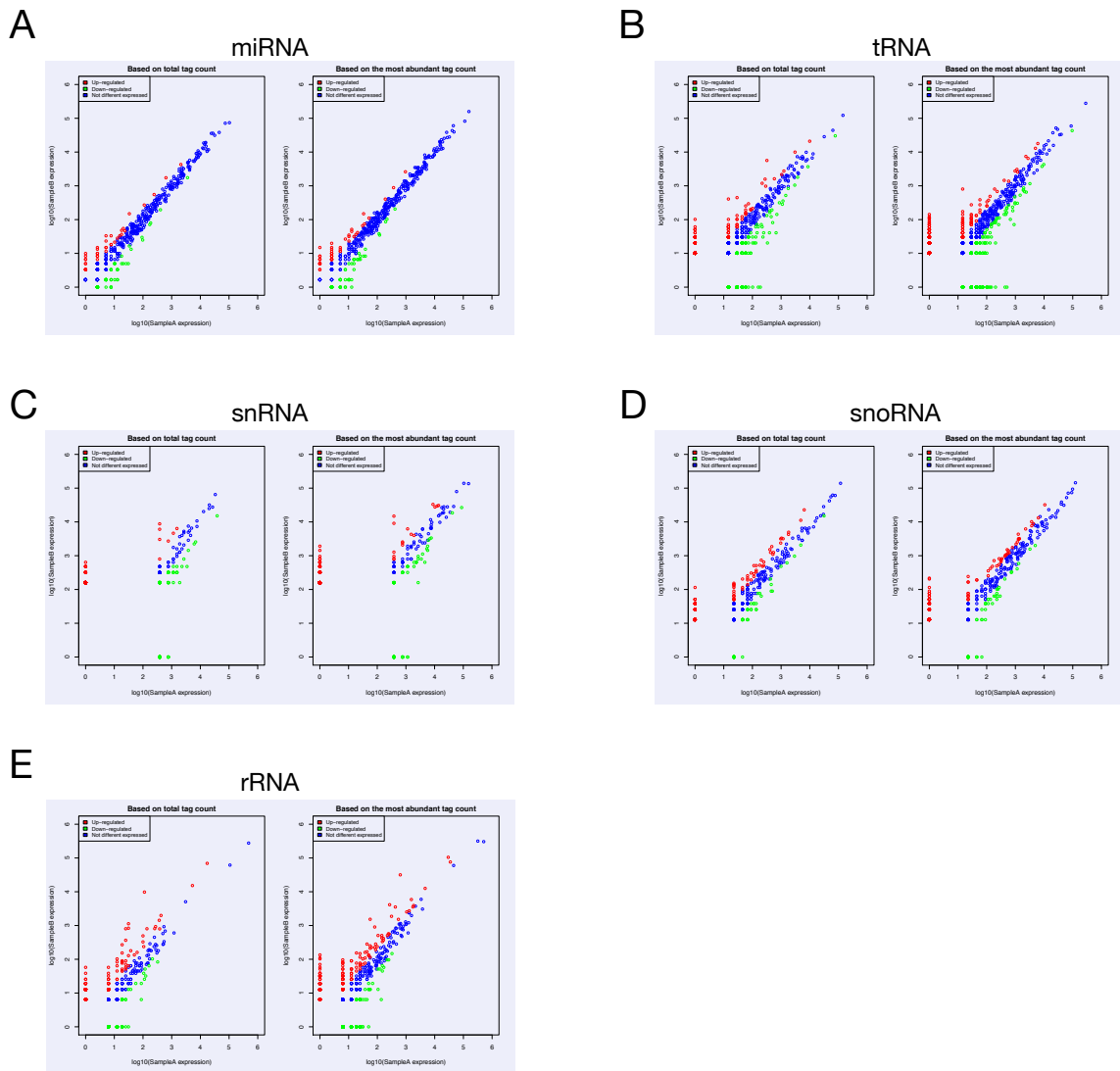


Figure 3.4. Changes in small RNA abundance due to nitrofen. Scatter blots represent the differential expression between nitrofen and control. Left panel: Based on total tag count (pre-normalization) and right panel: based on the most abundant tag count (post normalization) populations were presented for individual small RNA species. The X-axis represents the normalized expression levels of the control, and the scale is log 10. The Y-axis represents the normalized expression levels of nitrofen. Each point in the scatter represents an individual small RNA. The points on both sides on the diagonal line represent a ratio of the normalized expression of nitrofen/ the normalized expression of the control. SnRNA= Small Nuclear RNA, snoRNA=Small Nucleolar RNA.

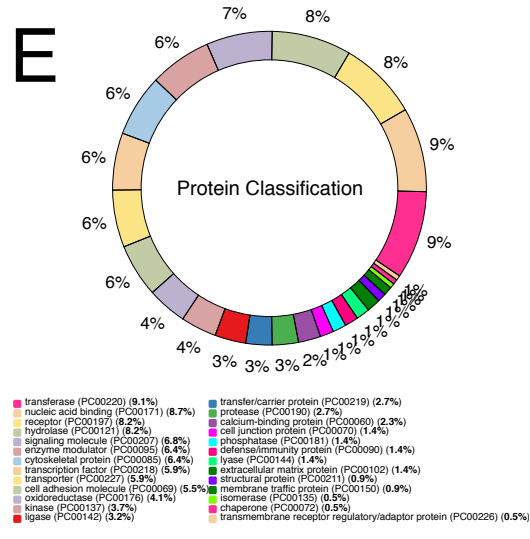
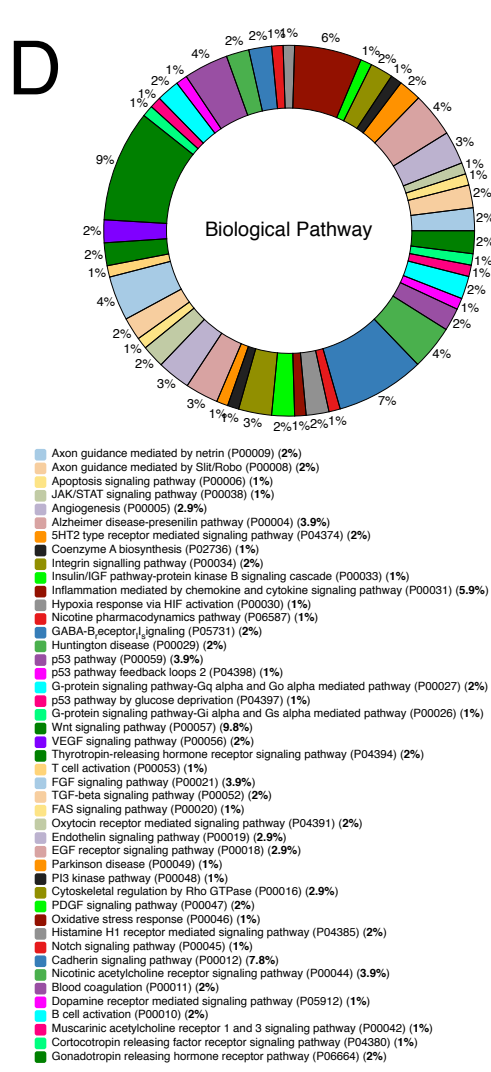
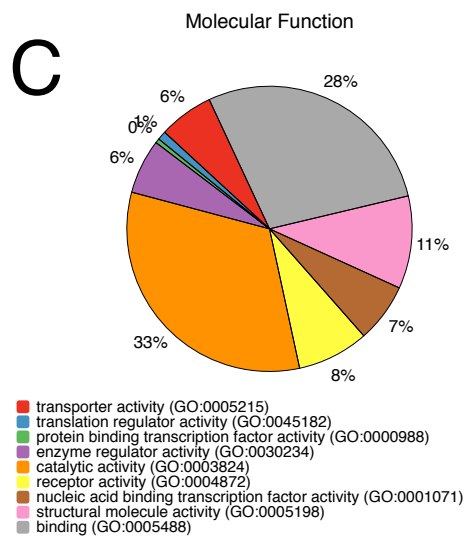
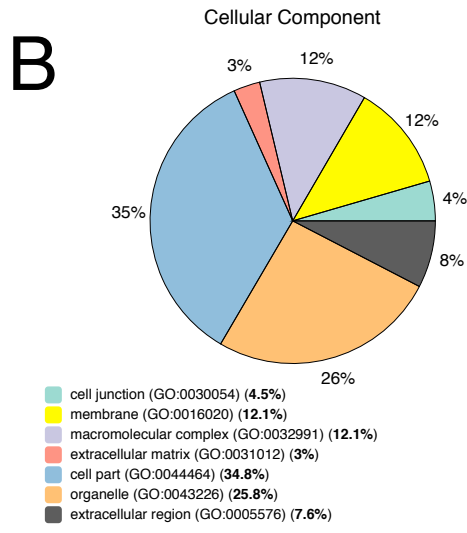
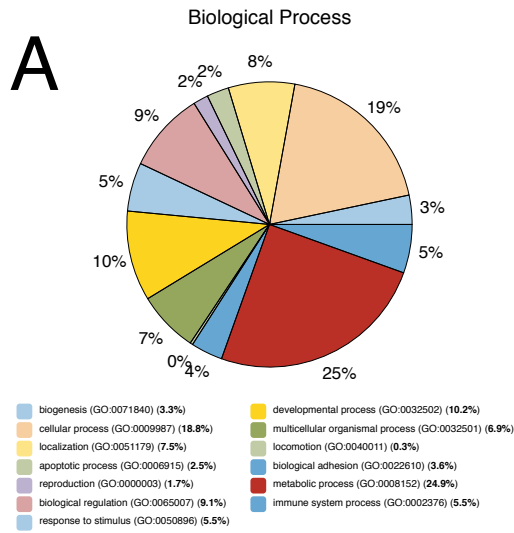


Figure 3.5. Transcript gene functional analysis was conducted using the PANTHER GO database. GO has been categorized into A) biological processes, B) cellular components, C) molecular function, D) biological pathways, and E) protein classification (191).

<p>mir-125-2/10 SCORE=28 Nseq=77 Len=186</p>	<pre> Mmus_42553 ACG-----AGACUUUGCCUAGUCCUGAGACCCU--AACUUGUG-A-GG-UA---U-UU-UAGUA-ACAUCACAAGUCAGGUUCUGGG-ACCUAGGGGGAGG-----GAU Mmus_19765 UG-----CGUCCUCCUAGUCCUGAGACCCU--AACUUGUG-A-UG-UU---U-ACC GUU-UAAAUCCACGGGUUAGGCUCUGGG-AGCUCGGGCGU-----GC Mmus_19717 U-----GCCGCCUCUGGGUCCUGAGACCCUUAACCUUG-A-GG-AC---G-U---CC-AGGGUCACAGGUGAGGUUCUGGG-AGCCUGGGCCU-----GCC Rnor_19718 U-----GCCGCCUCUGGGUCCUGAGACCCUUAACCUUG-A-GG-AC---G-U---CC-AGGGUCACAGGUGAGGUUCUGGG-AGCCUGGGCCU-----GCC Rnor_19764 UG-----CGUCCUCCUAGUCCUGAGACCCU--AACUUGUG-A-UG-UU---U-ACC GUU-UAAAUCCACGGGUUAGGCUCUGGG-AGCUCGGGAGUCU-----GC Rnor_19804 ACC-----AGACUUUCCUAGUCCUGAGACCCU--AACUUGUG-A-GG-UA---U-UU-UAGUA-ACAUCACAAGUCAGGCUCUGGG-ACCUAGGGGAGA-----GG Hsap_42548 ACC-----AGACUUUCCUAGUCCUGAGACCCU--AACUUGUG-A-GG-UA---U-UU-UAGUA-ACAUCACAAGUCAGGCUCUGGG-ACCUAGGGGAGA-----GGA Hsap_9524 U-----GCCGUCUCUAGUCCUGAGACCCUUAACCUUG-A-GG-AC---A-U---CC-AGGGUCACAGGUGAGGUUCUGGG-AGCCUGGGUCU-----GCC Hsap_40537 UG-----CGUCCUCCUAGUCCUGAGACCCU--AACUUGUG-A-UG-UU---U-ACC GUU-UAAAUCCACGGGUUAGGCUCUGGG-AGCUCGGGAGUCU-----G-----CU </pre>
<p>mir-142-142 SCORE=36 Nseq=25 Len=92</p>	<pre> Mmus_4073 -----ACCAUAAAAGUAGAAAGCACUACUA-ACAGCACUGGAG-GGUGUAGUGUUCCUACUUUAUGGAUG----- Rnor_77328 G--ACAGUGCAGUCAACCAUAAAAGUAGAAAGCACUACUA-ACAGCACUGGAG-GGUGUAGUGUUCCUACUUUAUGGAUGAGUGUACUGU-G Mmul_77325 G--ACAGUGCAGUCAACCAUAAAAGUAGAAAGCACUACUA-ACAGCACUGGAG-GGUGUAGUGUUCCUACUUUAUGGAUGAGUGUACUGU-G Ptro_77327 G--ACAGUGCAGUCAACCAUAAAAGUAGAAAGCACUACUA-ACAGCACUGGAG-GGUGUAGUGUUCCUACUUUAUGGAUGAGUGUACUGU-G Hsap_77326 G--ACAGUGCAGUCAACCAUAAAAGUAGAAAGCACUACUA-ACAGCACUGGAG-GGUGUAGUGUUCCUACUUUAUGGAUGAGUGUACUGU-G </pre> <p style="text-align: center;">* ***** * *****</p>
<p>mir-99/10 SCORE=36 Nseq=61 Len=120</p>	<pre> Mmus_19064 -----CCCAUUGCAUAAAACCCGUA GAUCCGAACUUUGUGUGAAG-UGG-----ACCGCAAGCUCGUUUCUAUGGGUCUGUG-GCAGUG-----UG Mmus_13429 C-----CUGUUGCCACAAAACCCGUA GAUCCGAACUUUGUGUG---AUUC-----UGCACACAAGCUCUGUUCUAUAGGUAUGUG-UCUGUUA-----GG Mmus_83027 -----GGCACCACCCGUA GAACCGACCUUGCGGGCCUUCGC-----CGCACACAAGCUCGUUUCUAUGGGUCCGUG-U-----C Rnor_83028 -----GGCACCACCCGUA GAACCGACCUUGCGGGCCUUCGC-----CGCACACAAGCUCGUUUCUAUGGGUCCGUG-U-----C Rnor_19125 C-----CUGUUGCCACAAAACCCGUA GAUCCGAACUUUGUGUG---ACCA-----UGCACACAAGCUCGUUUCUAUAGGUAUGUG-UCUGUUA-----GG Rnor_19061 -----CCCAUUGCAUAAAACCCGUA GAUCCGAACUUUGUGUGAAG-UGG-----ACCGCAAGCUCGUUUCUAUGGGUCCGUG-GCAGUG-----UG Hsap_71329 -----CCCAUUGCAUAAAACCCGUA GAUCCGAACUUUGUGUGAAG-UGG-----ACCGCAAGCUCGUUUCUAUGGGUCCGUG-UCAGUG-----UG Hsap_83024 -----GGCACCACCCGUA GAACCGACCUUGCGGGCCUUCGC-----CGCACACAAGCUCGUUUCUAUGGGUCCGUG-U-----C Hsap_45611 C-----CUGUUGCCACAAAACCCGUA GAUCCGAACUUUGUGUA---UUAG-----UCCGCAAGCUCGUUUCUAUAGGUAUGUG-UCUGUUA-----GG </pre> <p style="text-align: center;">***** **** **** *</p>
<p>mir-25 SCORE=36 Nseq=61 Len=120</p>	<pre> Mmus_19064 -----CCCAUUGCAUAAAACCCGUA GAUCCGAACUUUGUGUGAAG-UGG-----ACCGCAAGCUCGUUUCUAUGGGUCUGUG-GCAGUG-----UG Mmus_13429 C-----CUGUUGCCACAAAACCCGUA GAUCCGAACUUUGUGUG---AUUC-----UGCACACAAGCUCGUUUCUAUAGGUAUGUG-UCUGUUA-----GG Mmus_83027 -----GGCACCACCCGUA GAACCGACCUUGCGGGCCUUCGC-----CGCACACAAGCUCGUUUCUAUGGGUCCGUG-U-----C Rnor_83028 -----GGCACCACCCGUA GAACCGACCUUGCGGGCCUUCGC-----CGCACACAAGCUCGUUUCUAUGGGUCCGUG-U-----C Rnor_19125 C-----CUGUUGCCACAAAACCCGUA GAUCCGAACUUUGUGUG---ACCA-----UGCACACAAGCUCGUUUCUAUAGGUAUGUG-UCUGUUA-----GG Rnor_19061 -----CCCAUUGCAUAAAACCCGUA GAUCCGAACUUUGUGUGAAG-UGG-----ACCGCAAGCUCGUUUCUAUGGGUCCGUG-GCAGUG-----UG Hsap_71329 -----CCCAUUGCAUAAAACCCGUA GAUCCGAACUUUGUGUGAAG-UGG-----ACCGCAAGCUCGUUUCUAUGGGUCCGUG-UCAGUG-----UG Hsap_83024 -----GGCACCACCCGUA GAACCGACCUUGCGGGCCUUCGC-----CGCACACAAGCUCGUUUCUAUGGGUCCGUG-U-----C Hsap_45611 C-----CUGUUGCCACAAAACCCGUA GAUCCGAACUUUGUGUA---UUAG-----UCCGCAAGCUCGUUUCUAUAGGUAUGUG-UCUGUUA-----GG </pre> <p style="text-align: center;">***** **** **** *</p>

Source ([191](#)).

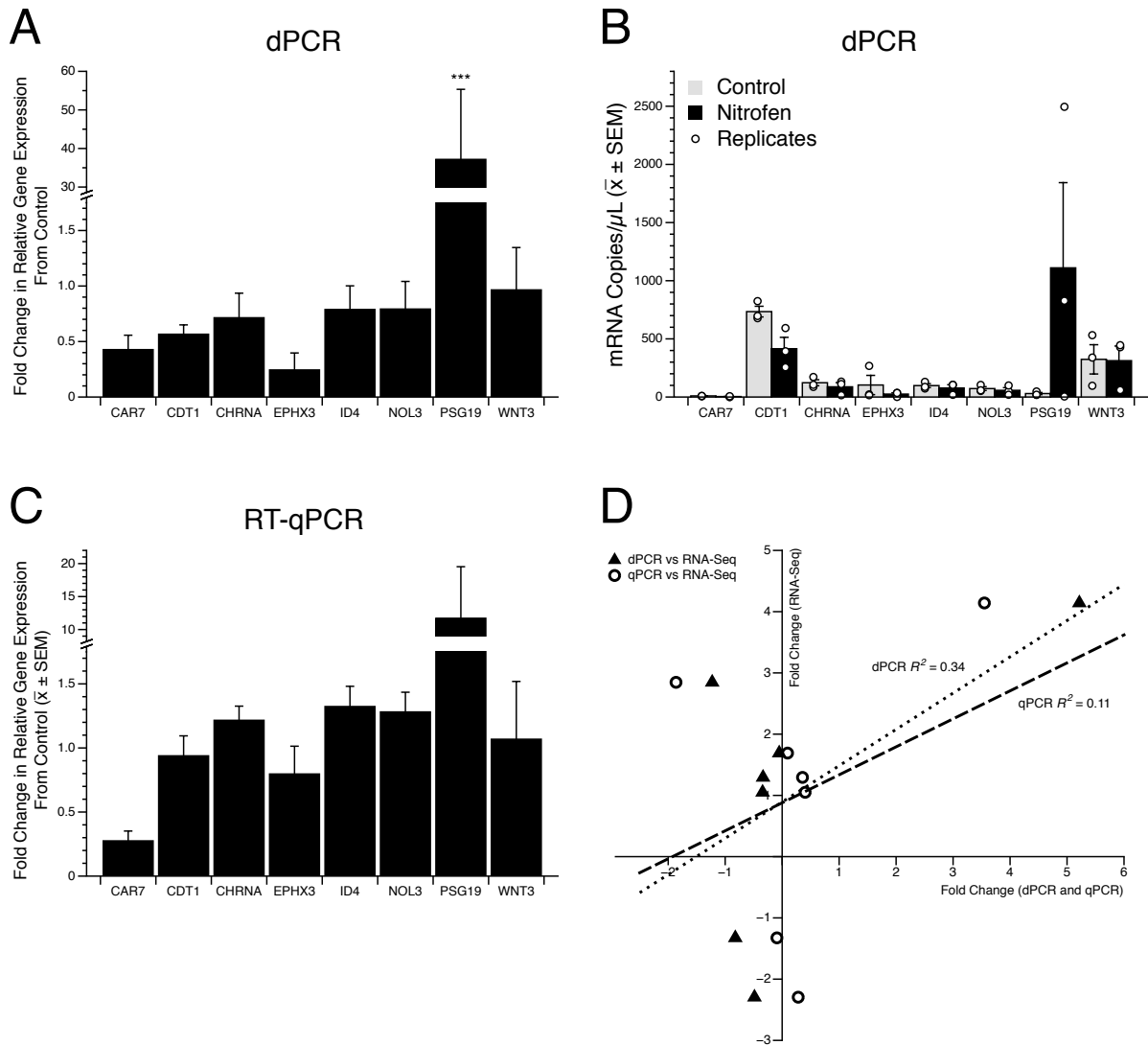


Figure 3.7. NGS Validation by dPCR and RT-qPCR. Validation of the expression of a subsample of genes by dPCR. Two-way ANOVA (***, $P < 0.001$) (A, B). RT-qPCR of the selected NGS transcripts with no significant changes were shown (PSG19 two tailed t-test ($P=0.0558$)) (C). (D) Linear regression correlation of RNA-seq (Y axis) with dPCR and qPCR data (X axis) using a log2 mean fold change measure of the genes differentially expressed across the two gene-expression platforms under correlation analysis. Outliers (Ephx3) were identified and removed as having 1.5 standard deviations or larger (191).

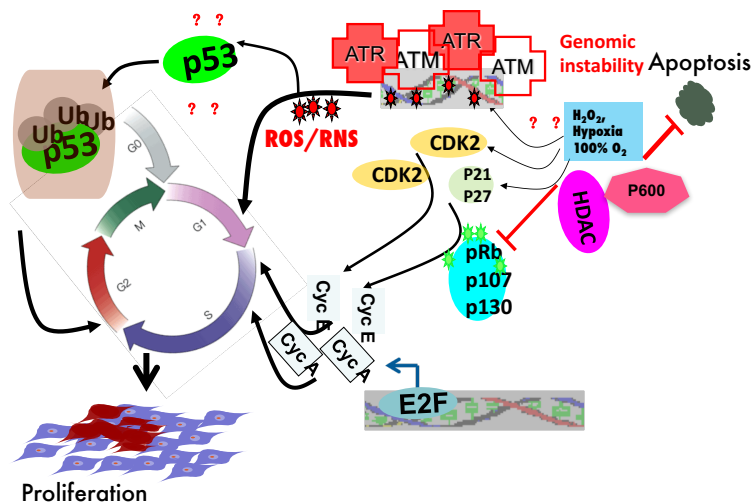


Figure 4.1. Hypoxia integrates with oxidative and nitrosative stress signaling to induce the cell cycle by a mechanism that is yet to be identified. p16, p21, and p27 are three CDKI that associate with and inactivate CDK, which results in growth arrest. Hypoxia promotes PASM proliferation by p27 protein degradation. p27 regulates SM proliferation in vitro. P27(Kip1) is a member of the Cip/Kip family of CDK inhibitors. p27 binds to G1 cyclin/CDK complexes (cyclin D/CDK4, cyclin E/CDK2, and cyclin A/CDK2) to inhibit their kinase activity and negatively regulate the cell cycle by blocking the cell at the G1:S transition. One of the mechanisms through which hypoxia maintains the proliferative ability include the E2F family of transcription factors, that is essential for cell cycle progression. Of the eight family members, E2F1, is a downstream effector of cell cycle regulators that plays a critical role in governing DNA synthesis. p27 is an upstream factor of E2F1, Cyclin D1 is downstream effector of p27 and upstream factor of E2F1 and is downregulated in PASM isolated from NHE1-deficient mice with decreased hypoxic PHN. E2F1 regulates CDK that are responsible for G1:S transition. NHE1 knockout significantly decreases the expression of Rho kinase 1 and 2. In hypoxia, what disrupts Rb-E2F complexes, resulting in the constitutive expression of E2F-responsive genes and promotes premature S phase entry and DNA synthesis is currently unknown. What hypoxia does so that it affects the expression of S phase genes by directly interacting with E2F factors is currently unknown. Normally p53 is required for p21 (Cip1) inhibition of cell cycle progression and transcriptional suppression of E2F gene activation of cell cycle progression. The Rb protein is a negative regulator of E2F1 and is controlled by the activity of upstream CDK that are activated during transition from Go:G1. ROS induce a DNA damage response that triggers DNA repair and cell cycle checkpoints, which in turn, maintain the integrity of the genome via p53 and Rb. P53 and Rb promote cell fates such as transient cell cycle arrest and DNA repair, cell death, that is, apoptosis, or permanent cell cycle arrest, that is, senescence or an imbalanced combination between apoptosis, senescence, and proliferation in the PHN SM. The induction of p21 and p27 results in Rb phosphorylation and Rb-E2F-mediated transcriptional repression. HDAC, histone deacetylase; Ub, ubiquitin (247).

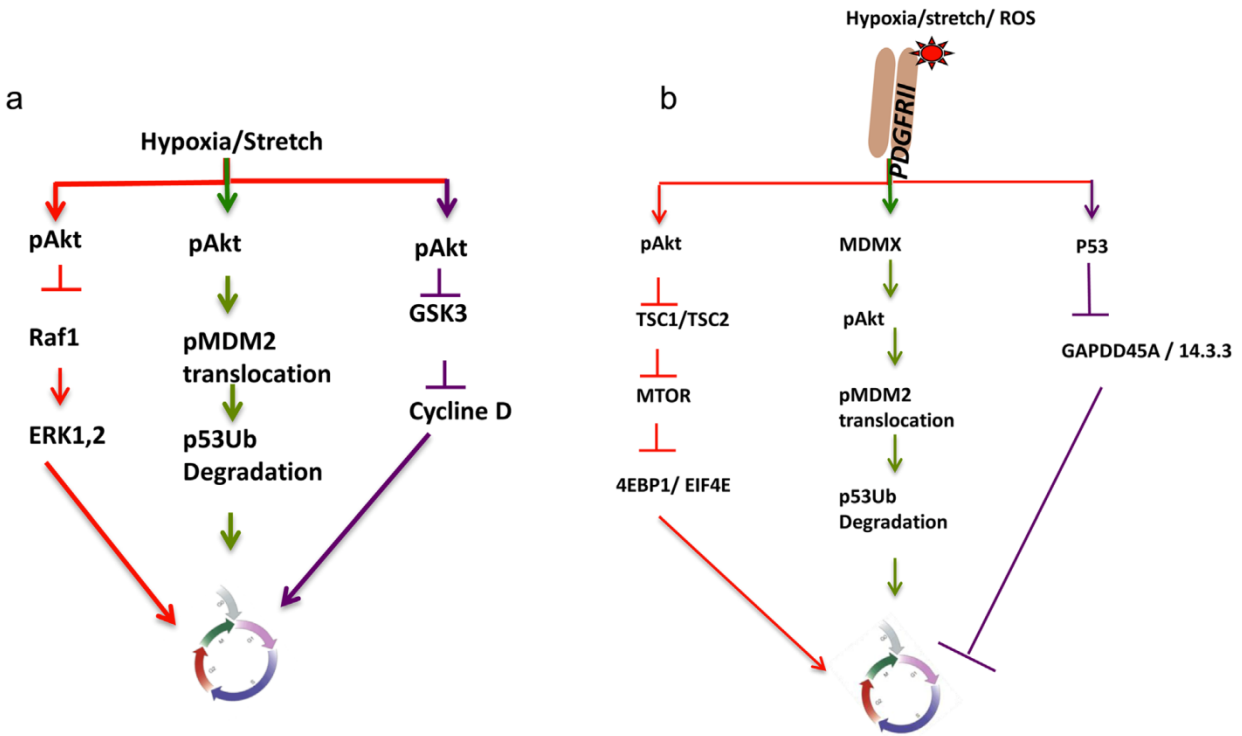


Figure 4.2. Putative models that may contribute to biomechanical signaling upstream of p53 are shown. (a) The AKT/MDM2 (Mouse double minute 2 homolog) model: Future investigations need to determine whether the phosphorylation of AKT triggers the activation and translocation of MDM2 to the nucleus and thus targets p53 for ubiquitination and degradation, which promotes cell cycle progression. The glycogen synthase kinase 3 (GSK) pathway is another putative pathway. Further investigations need to determine whether activation of AKT elicits inhibition of GSK3 and therefore the downregulation of cyclin D and cell cycle progression. (b) Future research is required to investigate the effect of hypoxia and stretch on the regulation of the TSC1/TSC2 (tuberous sclerosis) complex, which may elicit the mechanistic target of rapamycin (mTOR) inhibition and block eukaryotic initiation factor (eIF)4E-binding protein 1 (4EBP1/eIF4E) and protein synthesis and, thereby, indirectly affect G1:S transition. Downstream of platelet derived growth factor receptor B (PDGFRB), it is unknown whether MDMX upstream of AKT is activated, which eventually activates MDM2 to trigger p53 ubiquitination and translocation to the cytosol for degradation and promotion of death. The effect of hypoxia and stretch on growth arrest and DNA-damage-inducible protein GADD45 α (GADD45 α) and 14.3.3 may inhibit the G2:M transition downstream of p53 and arrest cell growth (247).

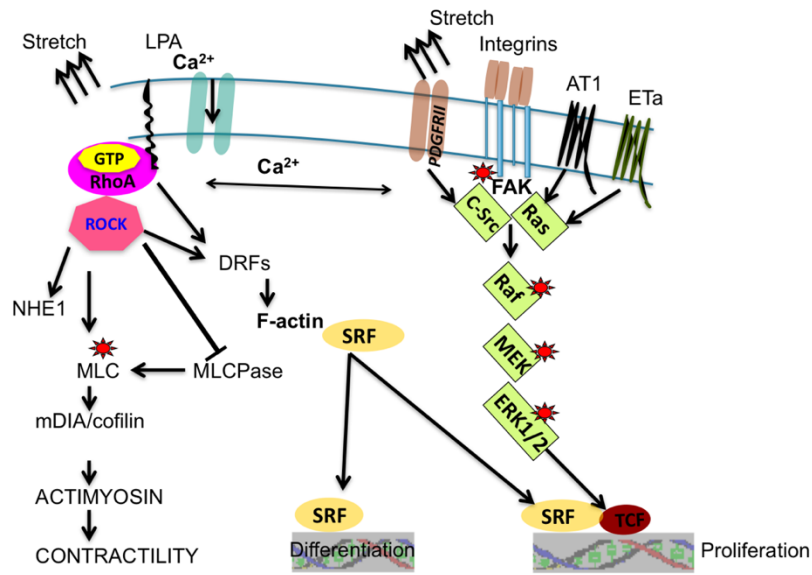
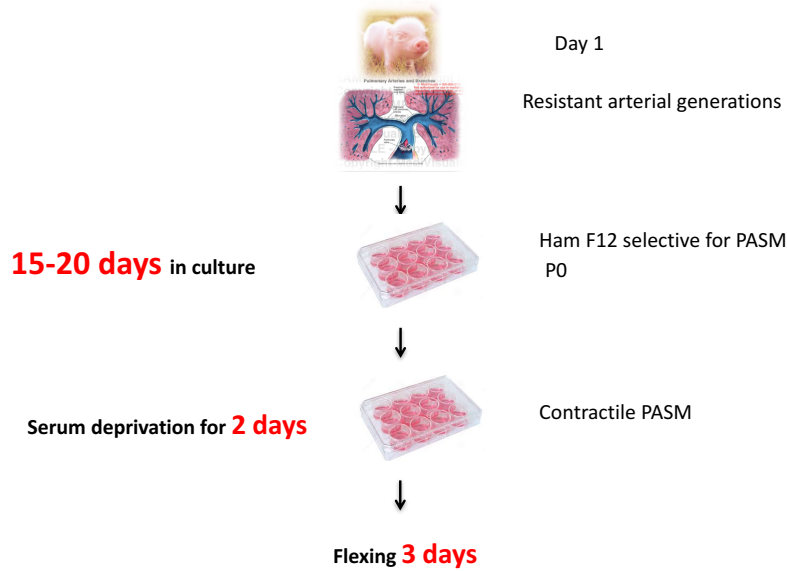


Figure 4.3. The small G protein coupled receptor (Rho) mediates the assembly and disassembly of actin filaments and ensures the integrity of the cytoskeleton which is essential for ERK-dependent gene transcription in response to stretch. Absence of stretch causes actin depolymerization, and loss of contractile phenotype, whereas growth factor stimulation of dissociated SM cells causes proliferation but with loss of contractility. Regulation of contractility and proliferation of SM by integrins and ET_A in normal vascular biology is shown. Mechanical forces are provided via interactions of extracellular matrix proteins with integrins in the cell membrane, activating the phosphorylation of FAK, which stimulates the rapidly accelerated fibrosarcoma RAF-MEK (MAP-ERK Kinase)-ERK 1/2 pathway and thus immediate early gene expression. Another cascade is triggered by factors that activate G protein coupled receptors (GPCR) such as angiotensin I (ATI), ET_A receptors, and tyrosine kinases, for example, PDGFR. Once phosphorylated, ERK is capable of entering the nucleus and phosphorylating ternary complex factors (TCF), which bind to SRF and activate the transcription of immediate early genes such as the transforming gene of the FBJ MSV (Finkel-Biskis-Jinkins murine osteogenic sarcoma virus), c-fos, and the putative transforming gene of avian sarcoma virus 17 (c-jun), and the early growth response protein 1 (Egr1). Integrins regulate the Ras homolog gene family, member A (RhoA) but how this regulation affects proliferation upon hypoxia and/or stretch has not been investigated. RhoA activation and its downstream effector Rho kinase were suggested in many studies to be involved in stretch-induced SM proliferation and inhibition of this pathway completely inhibited pulsatile stretch induced SM proliferation. Although the upstream signals responsible for the activation of Rho/Rho kinase signaling in mechanical hypoxic-induced PHN is unknown, this pathway is a convergent point for several vasoconstrictor signals such as those signals mediated by GPCR, receptor tyrosine kinase (RTK) and integrin clustering. Rho kinase inhibitors are more effective vasodilators in rat models of PHN, and this family includes compounds such as tyrosine kinase inhibitor Gleevec that inhibits PASM proliferation and reverses PAH in the monocrotaline and in chronic hypoxic injury rat models. Inhibition of Rho kinase inhibits ERK's translocation to the nucleus without affecting ERK's phosphorylation in SM. Both AT₂ and ET_A cause ERK phosphorylation in SM by a mechanism involving PKC and c-src (247).

A

PASM cells isolation



B

The in vitro model

	Normoxia Resting	21% O ₂ 72 HOURS	Serum deprived
	Normoxia + Flexing (control)	21% O ₂ 72 HOURS	± 5 % above the resting length (frequency 1.5 Hz) Serum deprived
	Hypoxia Resting	10% O ₂ 72 HOURS	Serum deprived
	Hypoxia + Flexing	10% O ₂ 72 HOURS	± 5 % above the resting length (frequency 1.5 Hz) Serum deprived

Figure 4.4. An *in vitro* model of neonatal PHN. (A) The method is PASM cell-specific. As collagenase disintegrates the ECM, non-muscle cells do not adhere in low Ca²⁺ conditions. Muscle cell isolation from the tissue does not seem to need high CaCl₂. A low gradient of CaCl₂ and F12-Ham is true optimal condition. (B) PASM cells from a newborn piglet are exposed to pulsatile stretch within a hypoxic or normoxic environment in tissue culture. Normoxic cells with the application of pulsatile stretch is the control state, while hypoxia in the absence of pulsatile stretch models the pulmonary hypertensive state ([247](#)).

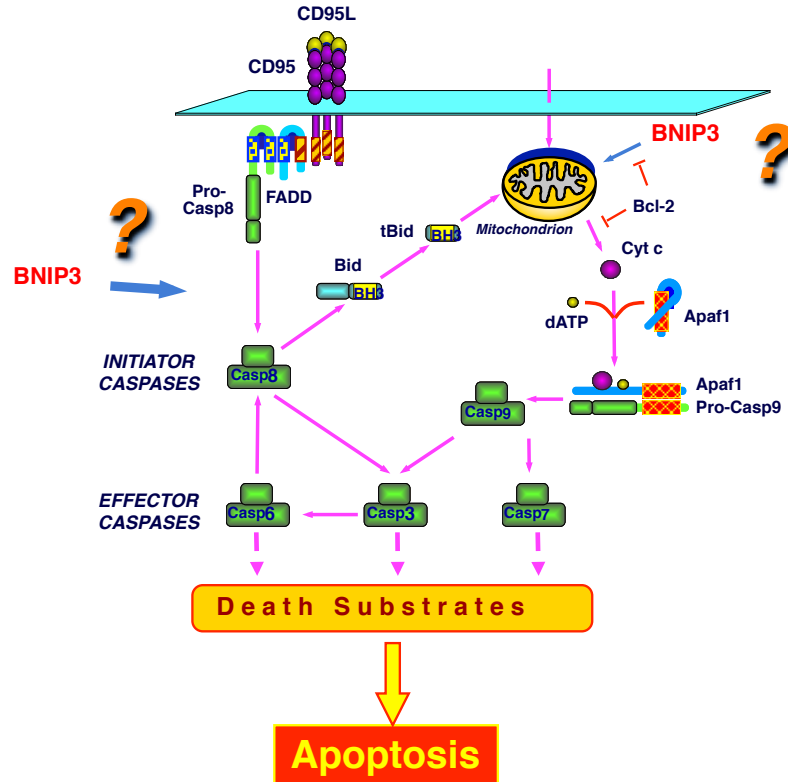


Figure 4.5. BNIP3 is a putative inducer of apoptosis. BNIP3 is a pro-apoptotic protein that interacts with viral anti-apoptotic proteins. The mammalian protein in *Homo sapiens* cDNA is 1,535 bp, of which the encoded protein is 194 aa, and the predicted molecular weight is 21.54 kD with a pI of 6.08; however, it migrates on the sodium dodecyl sulfate-polyacrylamide gels as a monomer of 30 kD and a homodimer of 60 kD. The BH3 domain contains Leu, Asp, and Ile as conserved residues. The BH3 domain of the Bcl2 family of proapoptotic proteins (Bik, Bid, Bim, Bax, and Bak) is essential for heterodimerization with antiapoptosis proteins. Examples include the following: adenovirus E1B 19 kD, Bcl2, Bcl-XL, *Caenorhabditis elegans* (CED-9), and Epstein-Barr virus (EBV)-encoded proteins (BHRF1) and targeting the green fluorescent heterologous protein GFP to the mitochondria. The carboxy terminus (31 aa) is required for the homodimerization as well as directing the expression to the mitochondria. All BNIP3 proteins contain PEST sequences. It is presumed that these proteins are degraded rapidly after expression in a stage-specific manner as a type of regulation to a lethal protein, and its degradation is controlled by the proteasome (247).

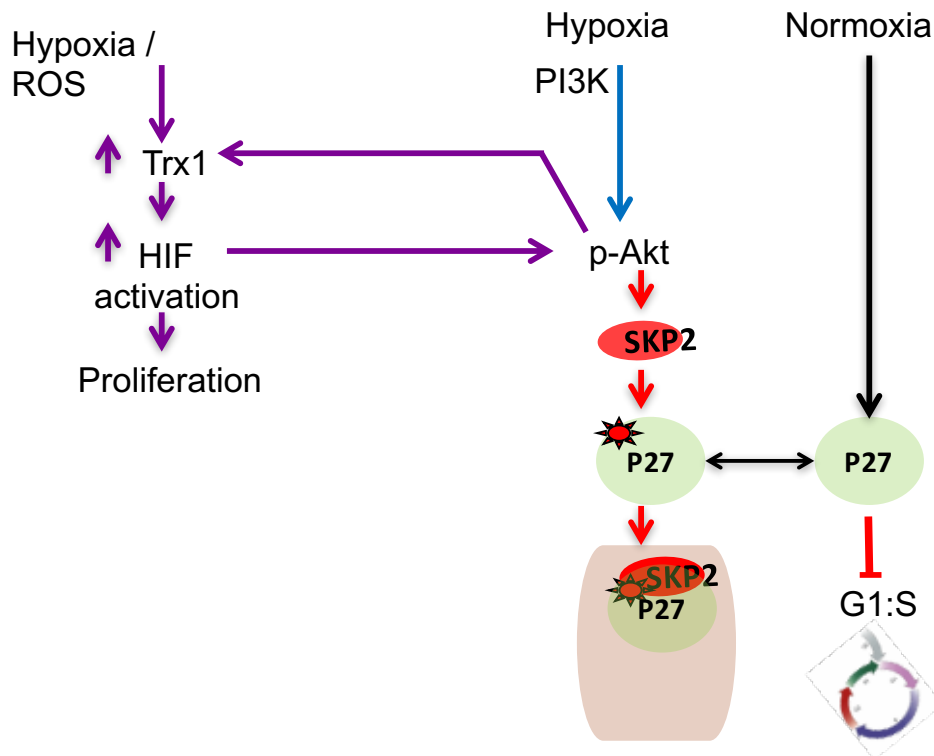


Figure 4.6. Hypoxia-induced PASM proliferation via the AKT/SKP2/p27-associated pathway. Hypoxia initiates PI3K signaling leading to AKT phosphorylation. The pro SKP2 acts in the ubiquitin-dependent proteolytic degradation of p27. The balance of cell proliferation and quiescence is regulated by p27 that inhibits G1 Cyclin/CDK complexes and blocks the cell in the G1:S. Trx1 is a redox protein disulfide reductase that links to AKT-dependent signaling in the mitochondria and cytosol. Nicotinamide adenine dinucleotide phosphate (NADPH) reduces and replenishes oxidized Trx1 from the disulfide to the dithiol state. Trx1 or its receptor TrxR1 are ubiquitously cytosolic, while Trx2 and TrxR2 are predominantly mitochondrial. Trx1 is a redox-dependent transcription factor for HIF-1 α . HIF-1 α is strongly implicated in PHN pathogenesis. Oxidative stress induced by hypoxia results in hydrogen peroxide (H₂O₂), which causes nuclear accumulation of Trx1. Upregulated Trx1-dependent HIF-1 α signaling promotes proliferation with downstream effects on PI3K-AKT signaling in both basal and hypoxia-induced PASM. This effect is dependent on O₂ tension. This model represents the importance of p27 as key regulator of PASM proliferation through the hypoxia/PI3K/AKT pathway which links hypoxia and ROS to cell cycle activation. Skp2, S-phase kinase-associated protein 2 (247).

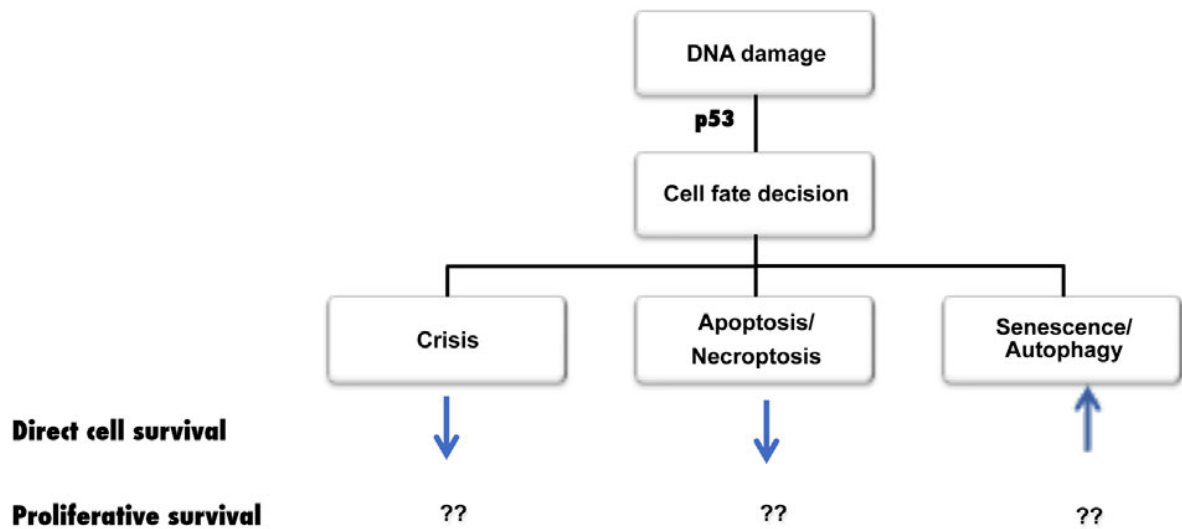


Figure 4.7. Correlation between resistance to therapy and cell fate decision is shown. Cell lines that commit to senescence can be used to assess direct and proliferative cell survival. Direct (96 hr) and proliferative cell survival (2–3 weeks) post-exposure to stressors reflect the ability of cells to survive the damage and to proliferate. The correlation between individual cell fates with direct or proliferative survival demonstrates if senescent SM cells have the potential to impact treatment outcomes. By comparing the proportions of direct cell survival with proliferative cell survival, it is possible to predict the cell fate taking into account the physiological conditions of the cell. The results will allow prediction of patient care through a better characterization of patient responses to current therapies and to design novel bioassays to search for small chemicals or cytokines that potentiate the senescence antiproliferative mechanism for future therapies (247).

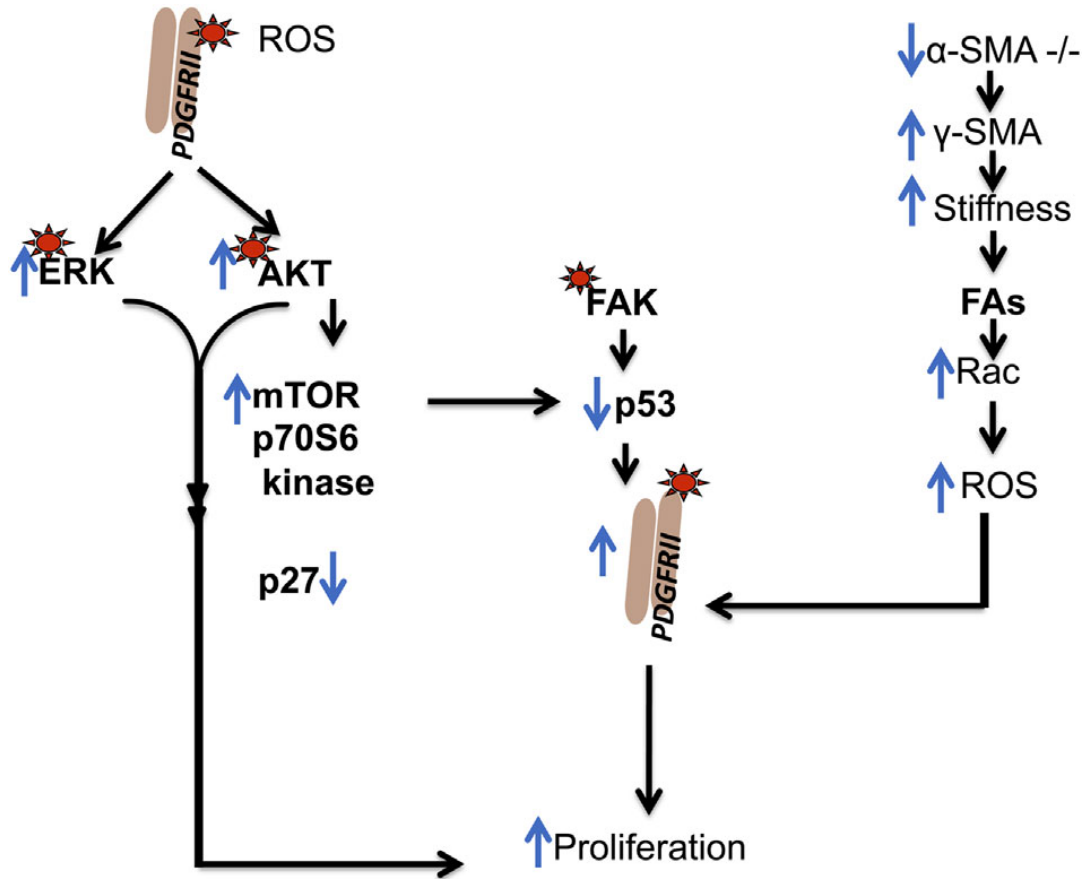


Figure 4.8. The link between the distribution of SM α -actin and SM hyperplasia in vascular diseases was studied by Papke et al (330) who used cells from SM-actin 22^{-/-} mouse. The group reported crosstalk between PDGFRB upregulated expression and activity. Activation of FAK and altered p53 localization caused SM hyperplasia in response to the loss of SM α -actin. In the actin null mutant cell, tension increases and activates FA maturation related to size and activity and influences their redistribution at the cell periphery compared to wild-type mice in which they were dispersed across the cell. SM-actin 22^{-/-} induced FAK (phosphorylated on Tyr297) was sufficient to suppress Rho and activate Ras-related C3 botulinum toxin substrate 1 (Rac1) independently upon Lysophosphatidic acid (LPA) stimulation, which induced proliferation mediated by increased ROS. Loss of SM-actin reduced p53 nuclear localization and increased PDGFRB expression and phosphorylation by a mechanism that involved FAK and mTOR activation, which increased the activation of PDGFRB. Upregulated mTOR was associated with increased phosphorylation of p70S6 kinase and abolished p27 activity indicative of AKT activation. In the same model, ROS-activated ligand-independent activation of PDGFRB occurs via the inhibition of the protein tyrosine phosphatase responsible for deregulating the active receptor (247).

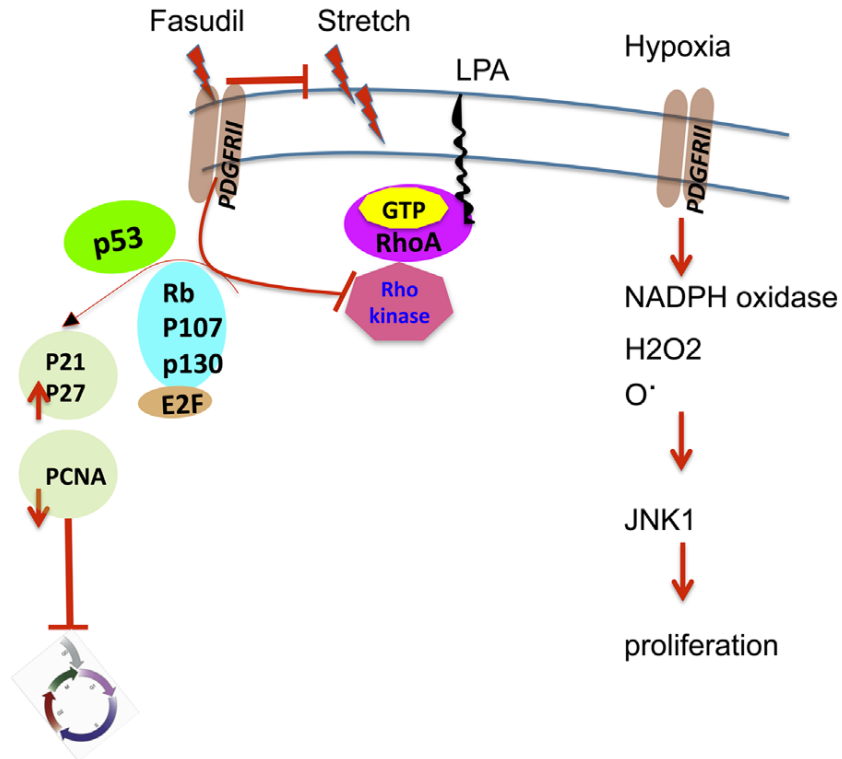


Figure 4.9. Chronic hypoxia elevates PDGFRB phosphorylation and activation is associated with PHN, specifically, hypoxia induces adventitial fibroblast proliferation by activating PDGFRB/JNK1 signaling that is mediated by modest elevation of NADPH oxidase-derived H₂O₂ and O^{•-} radical formation. The Rho/Rho kinase pathway contributes to growth factor-induced SM proliferation. Stretch-induced SM proliferation involves PDGF expression. Cyclins/CDK complexes regulate proliferation by phosphorylating and inactivating the transcriptional repressor Rb and allowing the expression of genes that trigger cell cycle progression. P16, p21, and p27 are key regulatory CDKIs. Normally, PDGFRB activates Rho kinase. In this model, the Rho kinase inhibitor fasudil (the only clinical available selective Rho kinase inhibitor that also functions as an intracellular Ca⁺² blocker) inhibits PDGFRB induced Rho kinase activation, and in turn elicits the activation of p21, p27 and downregulation of PCNA and growth arrest. Regulation of Rho inhibitor activity can be modulated by (i) arachidonic acid and protein oligomerization, which induces N-terminal transphosphorylation; (ii) RhoA upregulation of Rho kinase; (iii) the binding between the C-terminal of the Rho-binding domain to the N-terminal domain of Rho inhibitor inhibits Rho kinase activity. The p21 promoter region is reported to be bound to G9a (histone lysine methyltransferase; an epigenetic mark for gene suppression, DNA methyltransferase I and histone deacetylase I), which regulates the cell cycle (247).

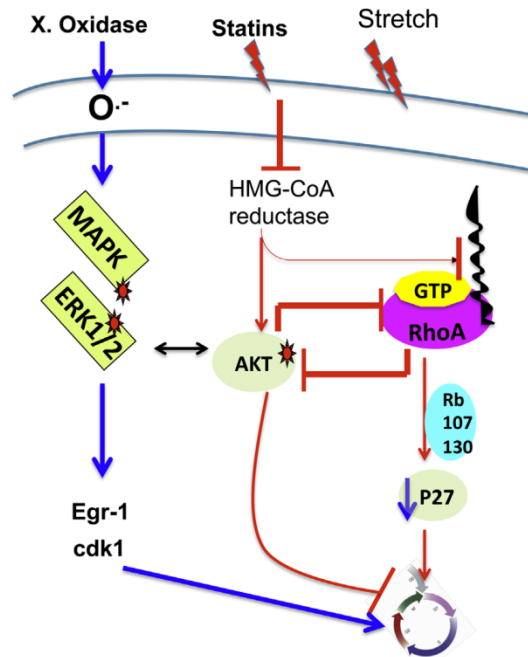


Figure 4.10. AKT is a serine/threonine kinase downstream of PI3K and is involved in cell survival and replication in SM. The PI3K/AKT pathway plays a critical role in vascular remodeling. Stretch increases the level of ERK1/2 and AKT phosphorylation. AKT phosphorylation positively regulates stretch-induced SM proliferation. Statins (cerivastatin and simvastatin) are used for the treatment of hypercholesterolemia. Statins prevent stretch-induced SM proliferation via inhibition of the RhoA/Rho kinase pathway in the saphenous vein by inducing the inhibition of mevalonate synthesis, which is a critical step in the synthesis and posttranslational modification of the geranyl-geranyl moiety that anchors Rho to the plasma membrane. Therefore, statins inhibit RhoA translocation to the plasma membrane and thus inactivate its binding to Rho kinase and prevent the downstream events. Cerivastatin significantly prevented stretch-induced membrane accumulation of RhoA, but not of P44/42 MAPK and AKT. Both activated AKT and inactivated RhoA have down regulatory effect on each other, but the mechanism is not well known. Mevalonate restored the preventive effect of cerivastatin on stretch-induced RhoA membrane accumulation. The effect of Rho inhibitors on the level of pAKT can be studied to demonstrate the crosstalk between Rho and AKT signaling and whether Rho/Rho regulates AKT. Whether the inhibition of RhoA is sufficient for the inhibition of stretch-induced proliferation in hypoxic PASM cells has not been studied. Rho/Rho kinase activation inhibits Rb, and Rho inhibitors and cerivastatin reduce Rb. Stretch-induced SM proliferation involves superoxide production and induces expression and translocation of Egr1. Egr1 is a redox-regulated early growth response transcription factor, it increases in the lung of neonatal pulmonary hypertensive calf in response to hypoxia, regulates downstream targets critical to proliferation and fibrosis and is implicated in vascular remodeling. The loss of extracellular SOD3 expression in cultured calf PASM cells mimics the hypoxia-induced extracellular ROS elevation observed *in vivo*. Xanthine oxidase (X. Oxidase) was given to the hypoxic PASM cells in culture. It was found that the loss of extracellular SOD was associated with an uprise of superoxide radical and this mediates up regulation of Egr1 via phosphorylation and activation MAPK/ERK1/2 and CDK1 activation ([247](#)).

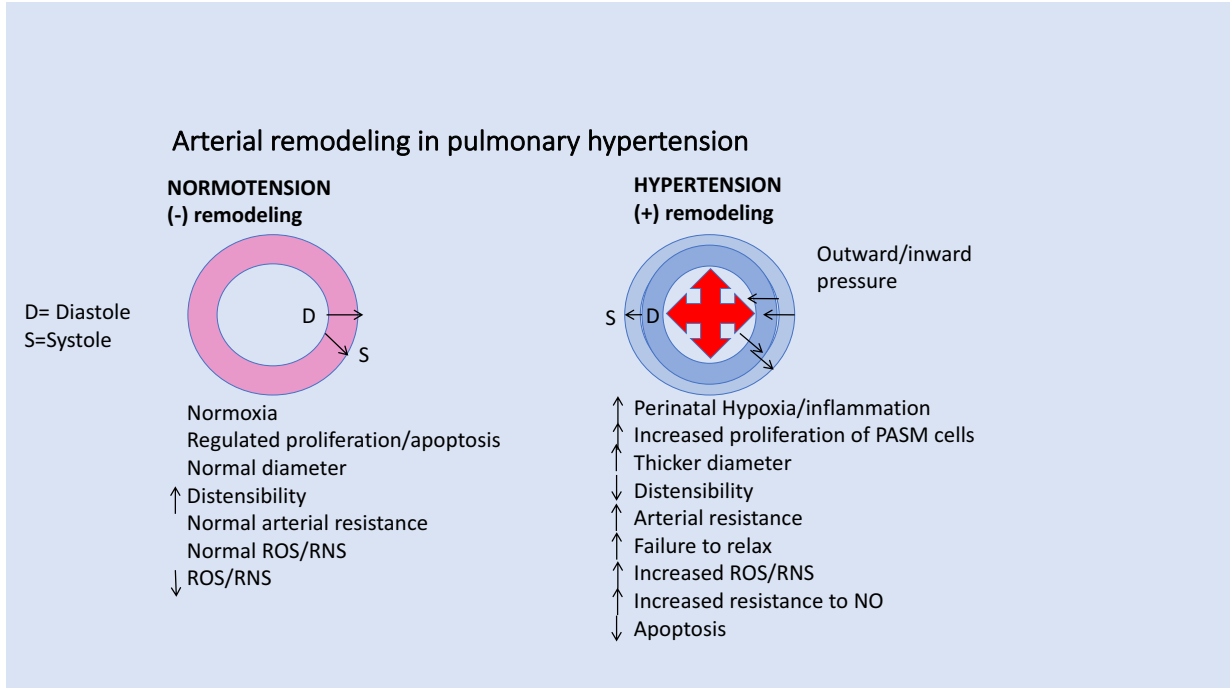


Figure 4.11. Arterial remodeling in persistent PHN. The perfusion in the pulmonary circuit depends on the cardiac effort (systole). One cardiac beat causes 10% stretch. In PH, one cardiac beat causes less than 10% stretch. The cytoskeleton reacts to stretch. With a small strain ($\pm 5\%$ from the resting length), there is heterogeneous response. With higher strain ($\pm 10\%$ from the resting length), a huge response occurs, such as a ripping damage to the cytoskeleton. High strain is associated with cell death due to the loss of adherence to the membrane. The arterioles change their diameter in response to local conditions such as sympathetic or endocrine stimulation. Capillary walls permit exchange of oxygen and metabolites between blood and the surrounding interstitial fluids. Diffusion distance is short and exchange is quick because the wall is thin. A high filamentous to monomeric actin (F:G) ratio increases stiffness, resulting in a thicker vessel diameter, higher pressure in remodeled versus non-remodeled vessels. Pulsation is non-harmonized due to the loss of distensibility. Remodeling is associated with HTN, higher ROS, and lower antioxidant enzyme levels (Catalase, SOD 1,2,3, Glutathione peroxidase, NADPAH oxidases (NOX)). Copyright is owned by Johar and Bernstein ([299](#)).

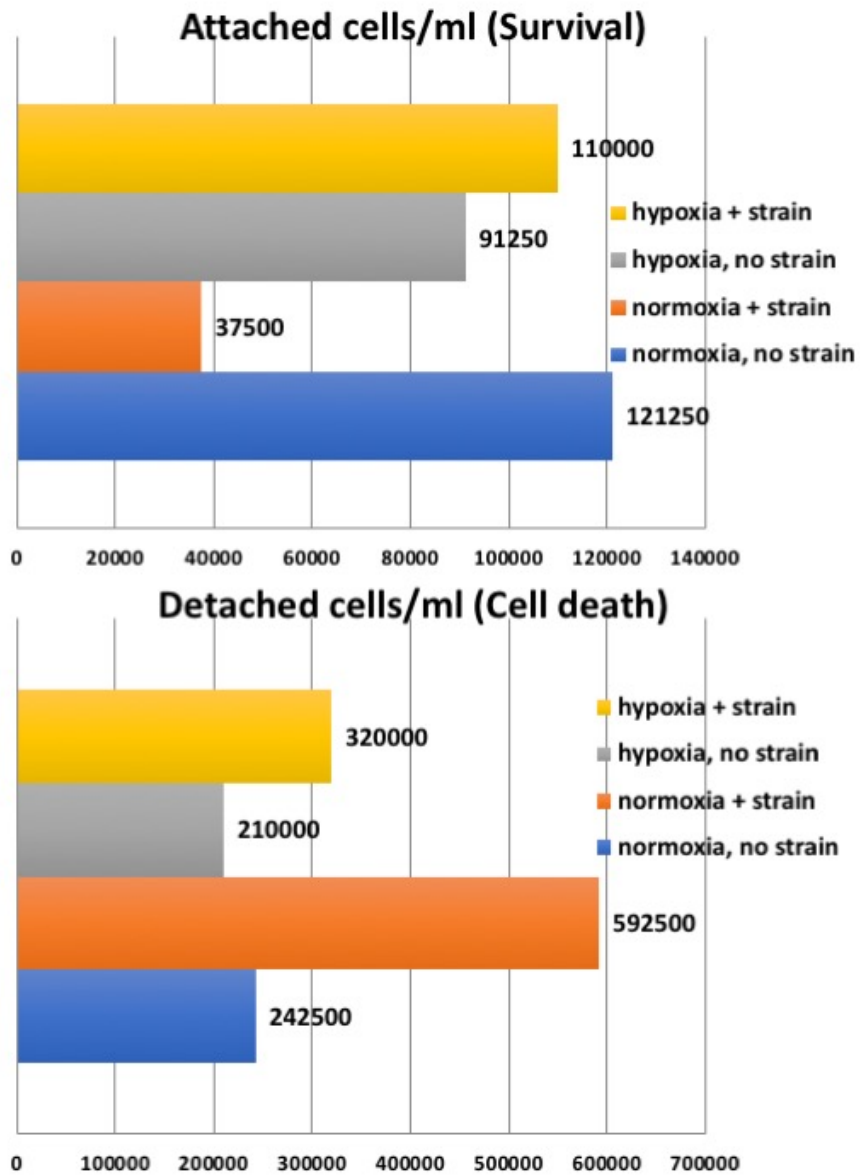


Figure 4.12. Cell count of the attached viable cells (upper) is compared to cell count of the detached dead cells (lower) graph. Seeding density is 70% prior to flexing in both experiments.

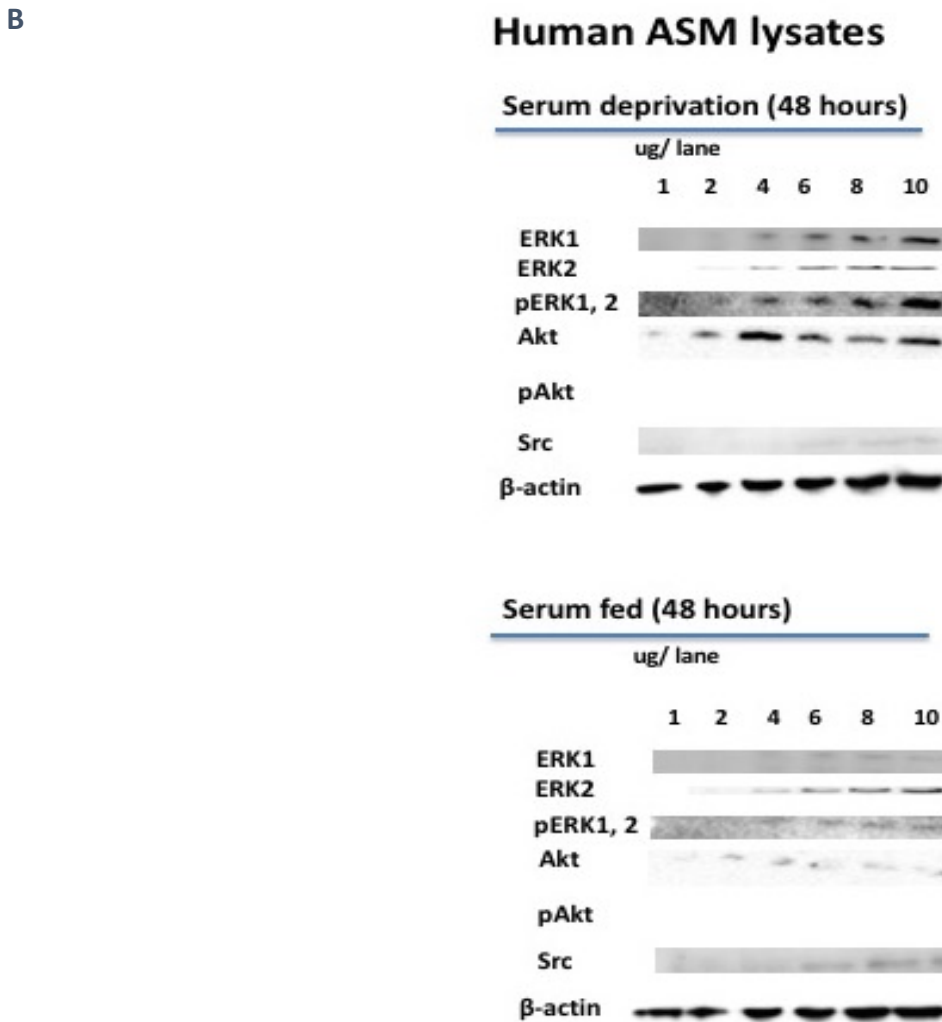
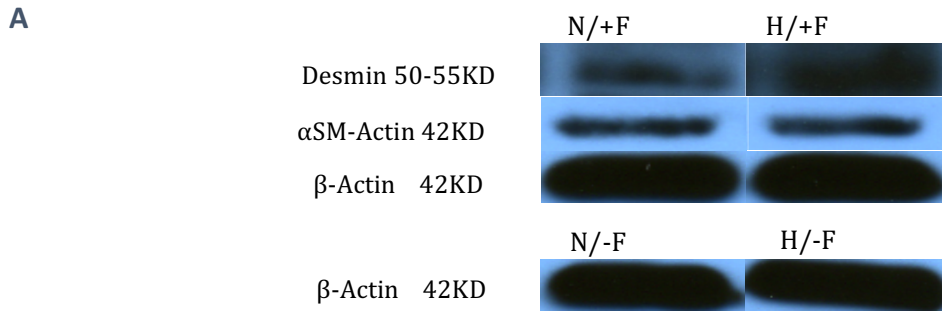
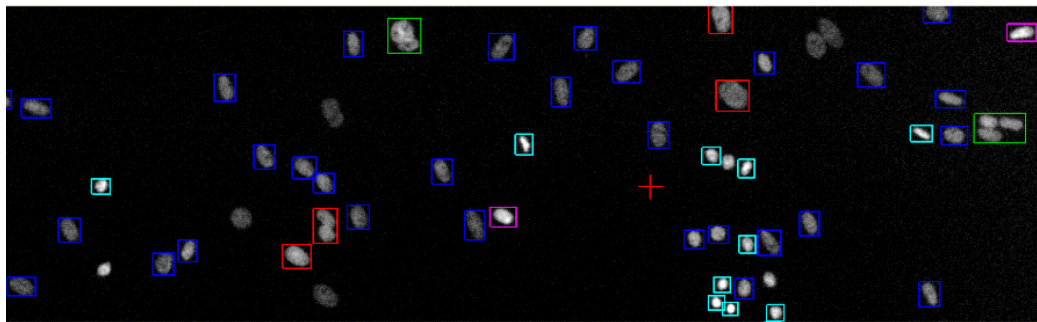
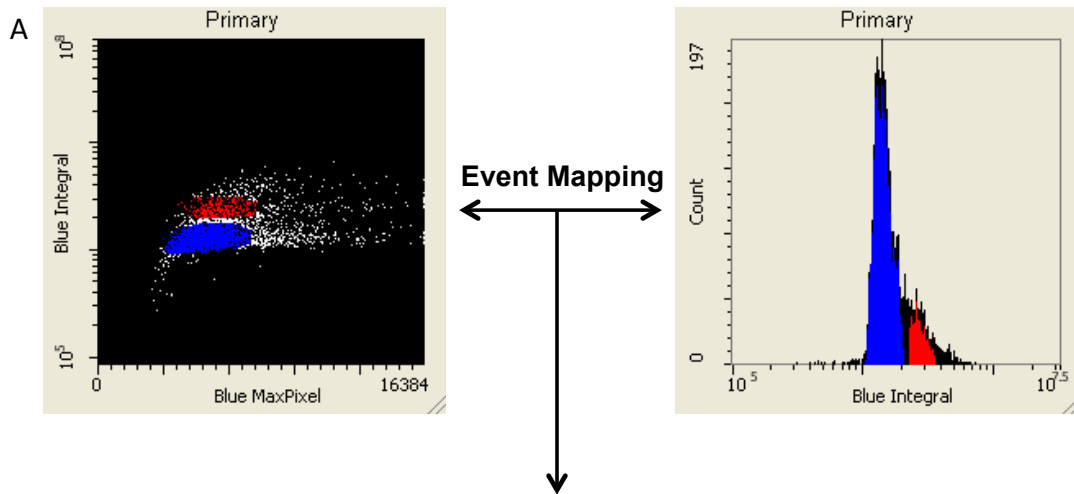
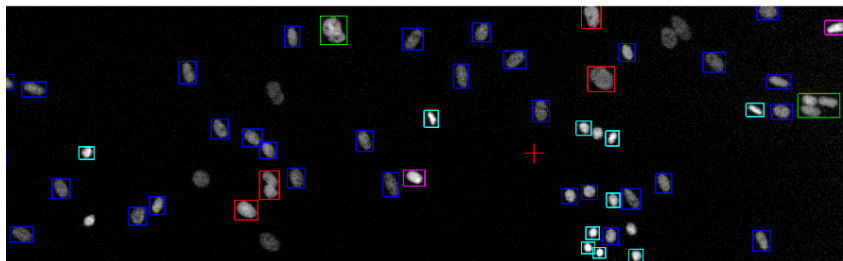
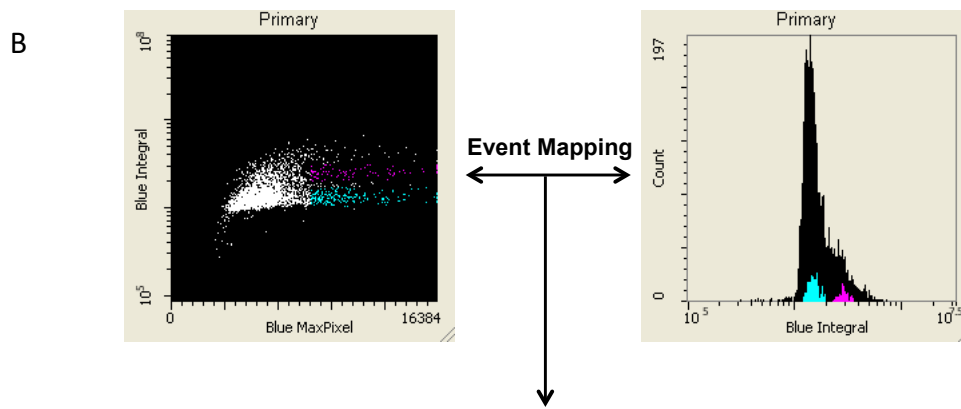


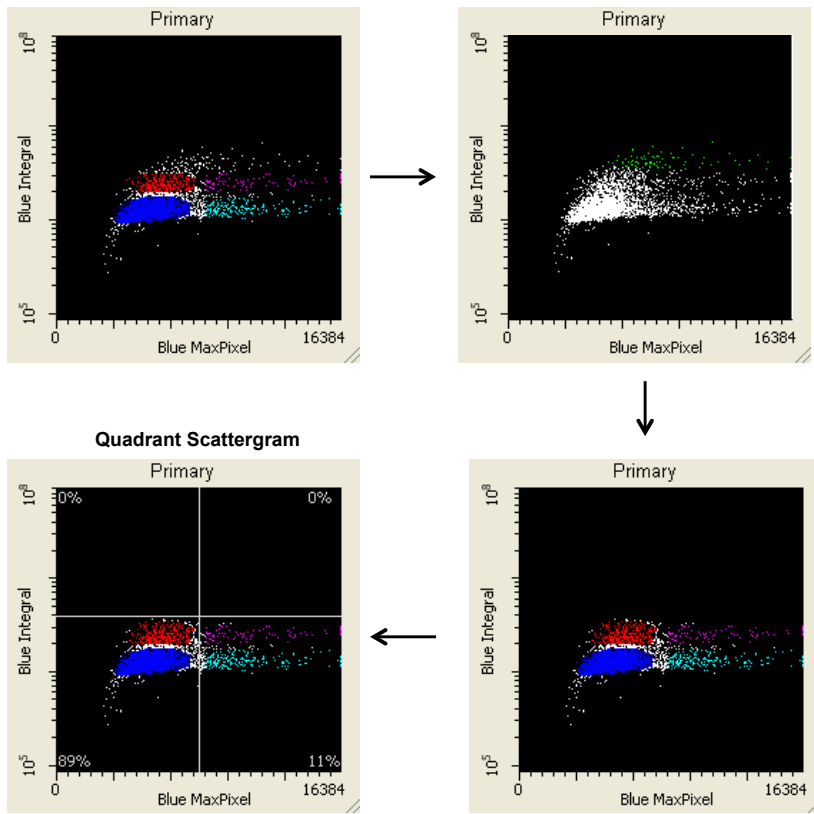
Figure 4.13. Examination of SM markers in hypertensive PASM (A) or normal hASM cells (B) to characterize the basal expression in SM cells. B) Levels of SM markers α -actin, β -actin, desmin in 20 μ g cell lysate in relation to different conditions of hypoxia and flexing. N= Normoxia; F=Flexing; H=Hypoxia. B) Concentration gradient shows the basal levels of ERK1/2, pERK1/2, AKT, src but not pAKT, as they are expressed in serum fed and serum deprived hASM. β -actin is a reference protein. Cropped gels are presented for both panels. Full-length gels and blots are shown in appendix A.



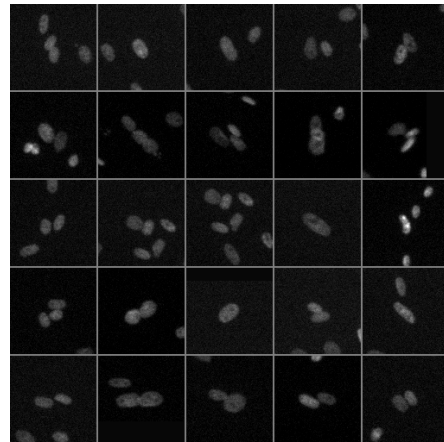
G0/G1 Events (Blue); G2 Events (Red)



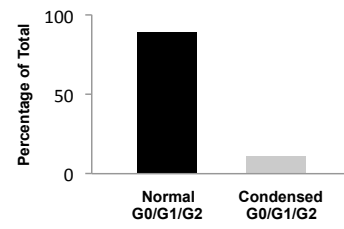
C



Gallery: Green Population



Cell Cycle Nuclear Events



D

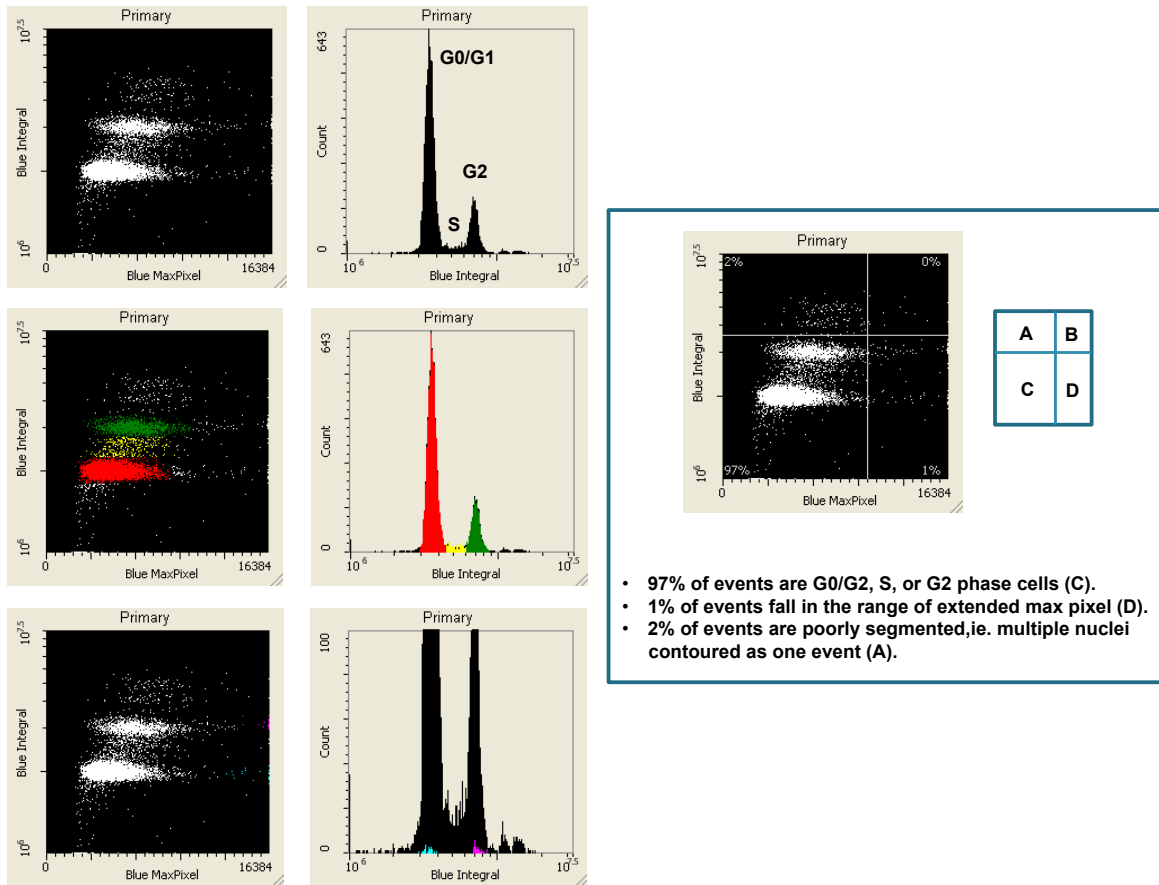
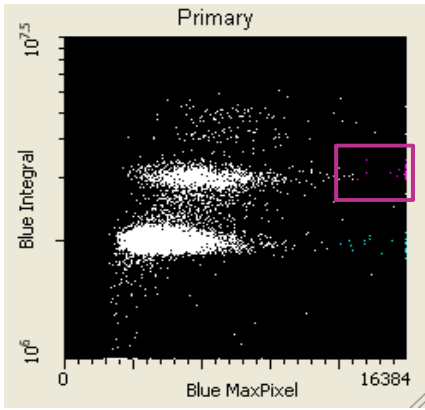
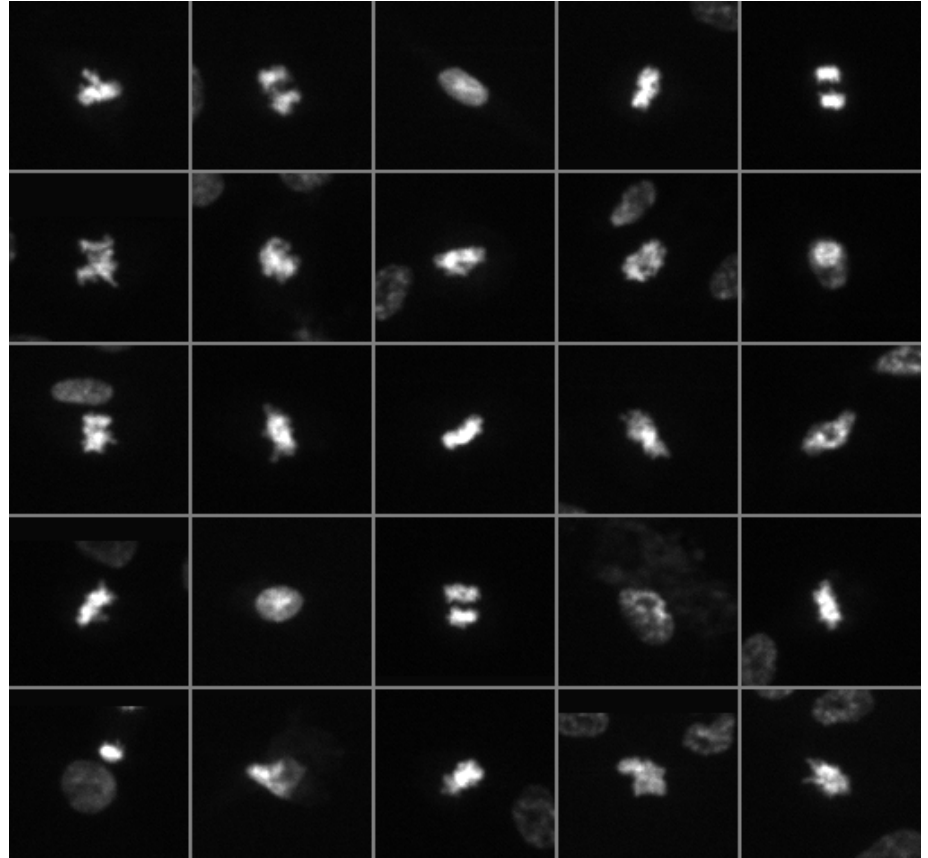


Figure 4.14. Cell cycle events. A) Event mapping of PASM cells, no treatment. Distinct event populations can be identified and colour coded within scattergrams or histograms and the colour-coded events mapped to their specific coordinates within recorded scan field images. B) Cell cycle events. Max pixel extensions of G0/G1 and G2 populations. Condensation of G0/G1 events is shown as cyan and of G2 events is in magenta. Nuclear condensation results in the cell cycle event populations with extended max pixel values in scatter gram plots. Nuclear condensation can be indicative of either mitotic or apoptotic processes. Event mapping shows that condensed nuclei have a morphology consistent with apoptosis occurring within the population of cultured cells. C) The horizontal/vertical division lines can be positioned manually, creating sectors of defined size (quadrants), D) the normal growing population in G0/G1 was predominant (97% of the total population).

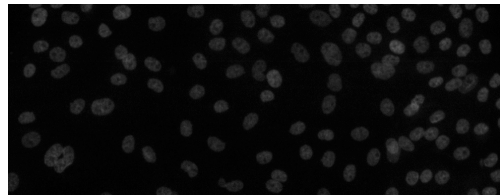
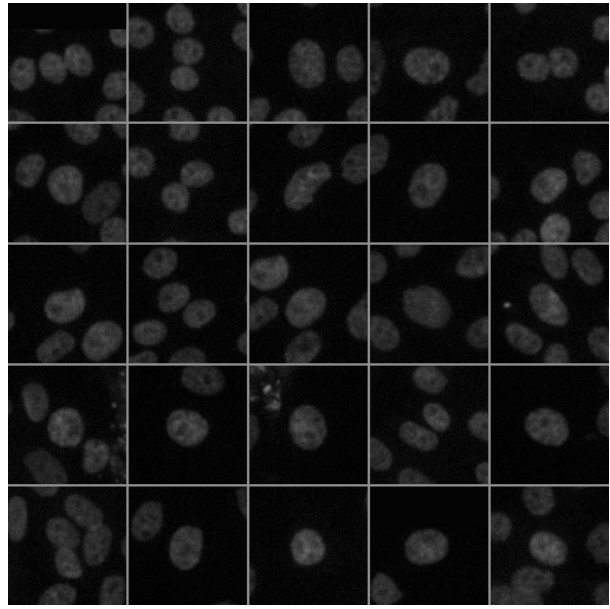
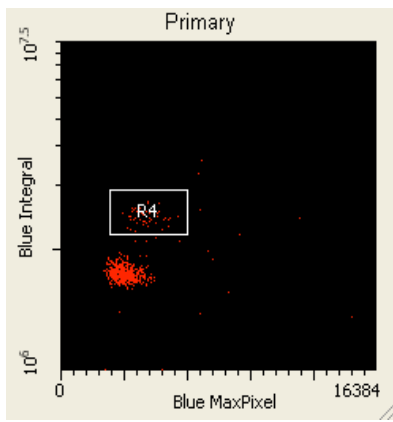
A

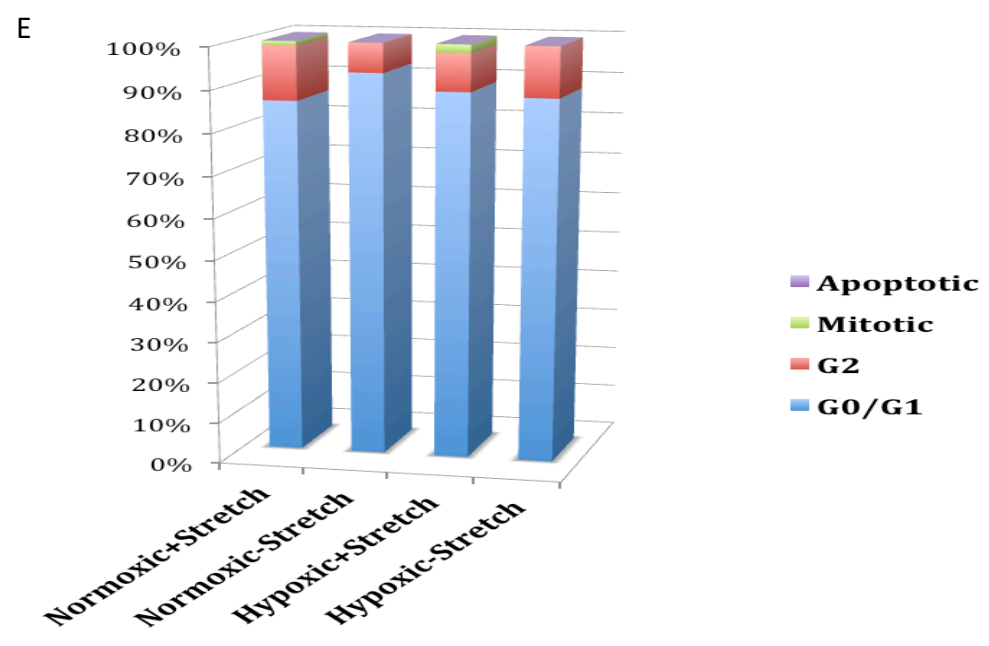
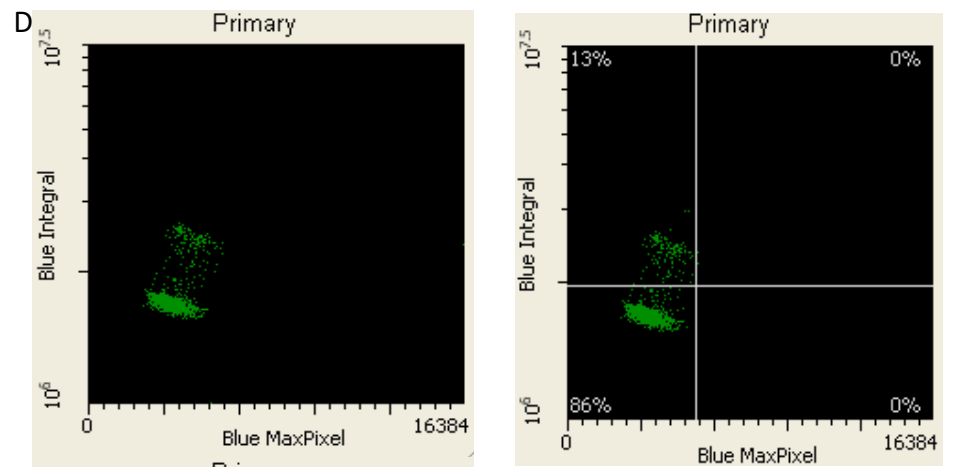
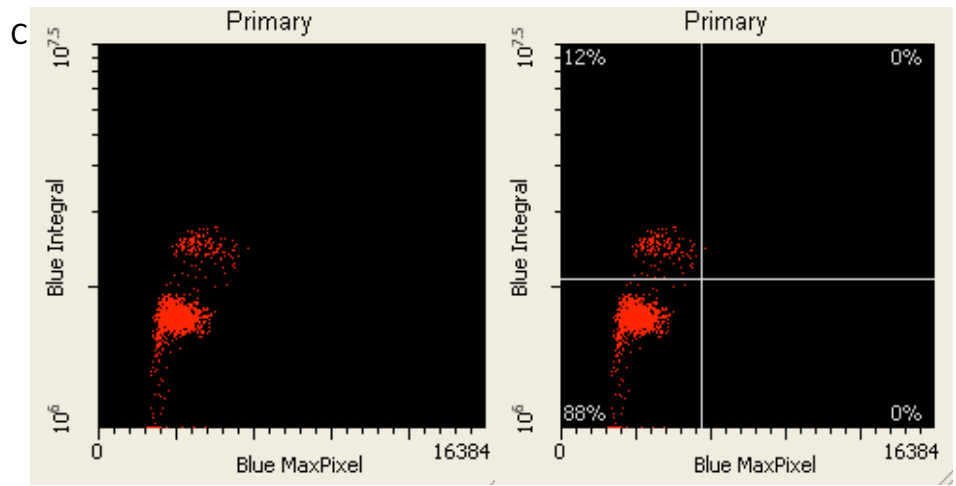


Majority of maxpixel events appear to be mitotic nuclei.



B





F	Well	Label	G2	G0/G1	Condensed G0/G1	Condensed G2
			Primary Count R5	Primary Count R6	Primary Count R8	Primary Count R10
	1		362	2,164	201	86

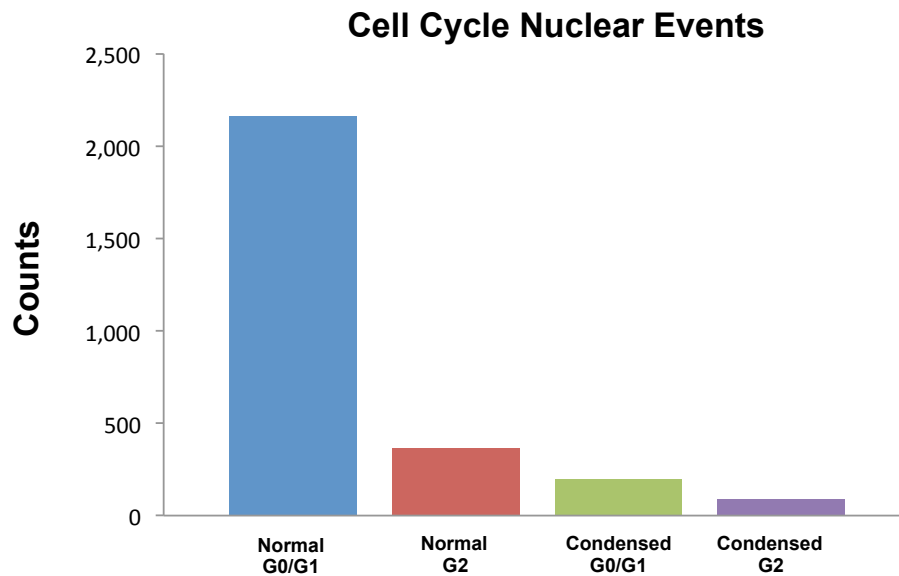
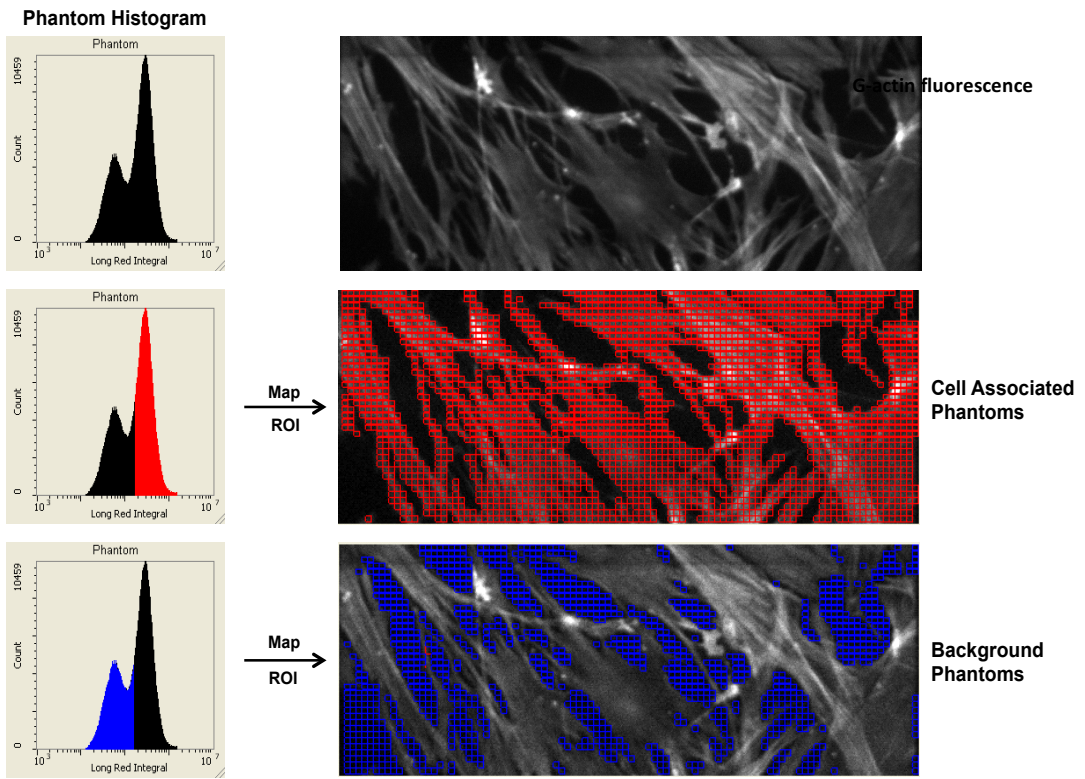
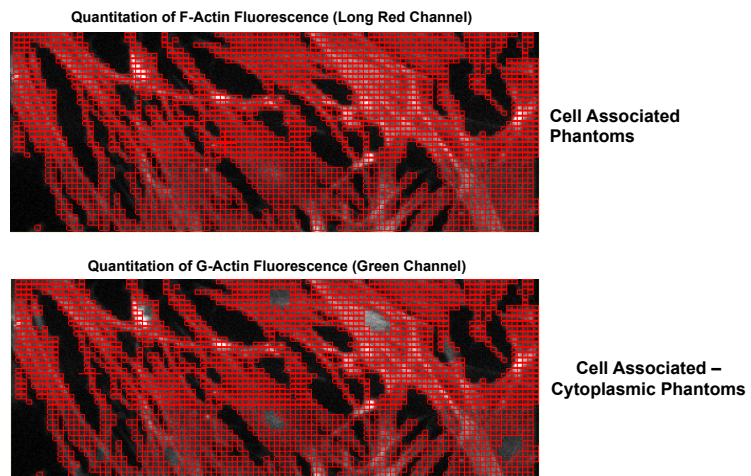


Figure 4.15. Quantification of cell cycle nuclear events by LSC. A) Gallery and field image of region 4 (R4) (G2 events). R4 is the region of interest (ROI). X, Y scattergram of hypoxia together with stretch representing regions of interest. B) Scattergram and quadrant statistics. Hypoxia without stretch; (The predominant proportion of normal cells is in G0/G1 phase 84% of total, and a small proportion is in G2 phase 15%. S phases: 1%. No apoptosis). C) Normoxia together with stretch. D) Normoxia without stretch. E) Apoptosis and cell cycle analysis. Hypoxia together with stretch: (G0/G1=88%, G2=12%, S=0%, apoptosis= 0%). Normoxia with stretch: (G0/G1 86%, G2 13%, M 1%). Normoxia without stretch: (G0/G1 93%, G2 7%). F) Statistics. The cytometer software contains a statistic package allowing for the selection of various statistical parameters for data analysis. For the present analysis, the statistical parameter "count" was used for the assessment of the percentage of nuclear events in various stages of the cell cycle. N=3 replicates.

A



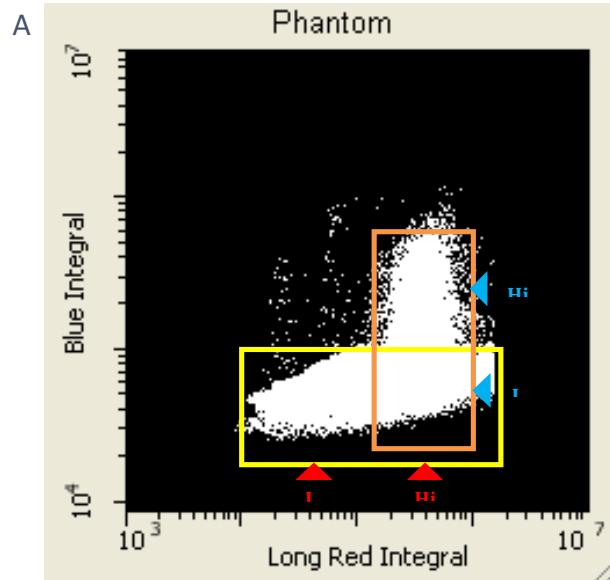
B



C

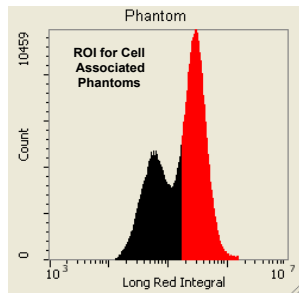
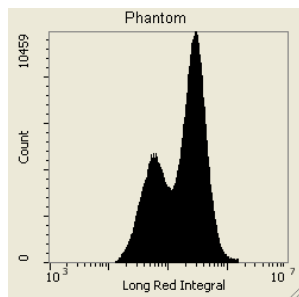
Phantom Integral Long Red Sum	Phantom Integral Green Sum	F-Actin/G-Actin Ratio (Sum)
74,520,809,222	23,094,202,036	3.2
Phantom Integral Long Red	Phantom Integral Green	
Mean	Mean	F-Actin/G-Actin Ratio (Mean)
344,232	111,163	3.1

Figure 4.16. Phantom contour analysis of cytoplasmic F:G-actin ratios in cultured primary PASM cells. A) Identification of background and cell associated phantom populations (long red channel). The cell associated phantom contour population is used for the quantification of F- and G-actin fluorescence. B) To remove the nuclear G-actin fluorescence from the total G-actin fluorescence, cell associated phantoms must be separated further into nuclear and cytoplasmic populations. This is achieved through a scattergram plot of blue versus long red phantom fluorescence, the numerical values of such separation are shown in C. C) Fluorescence quantification can be expressed either as the summed integrated fluorescence of all phantoms or as the mean integrated phantom fluorescence. ROI= region of interest.

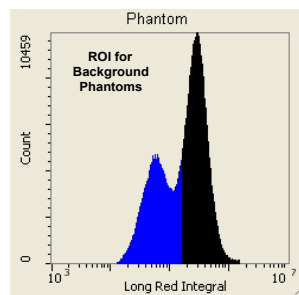
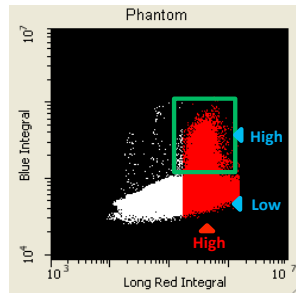
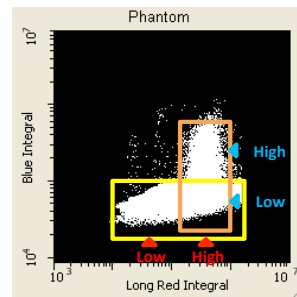


B

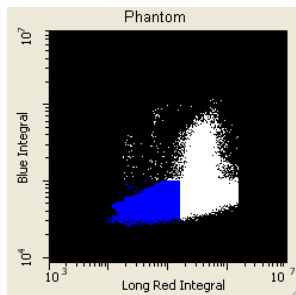
Phantom Histograms



Map to
Scattergram

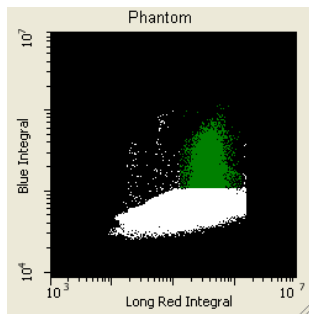


Map to
Scattergram

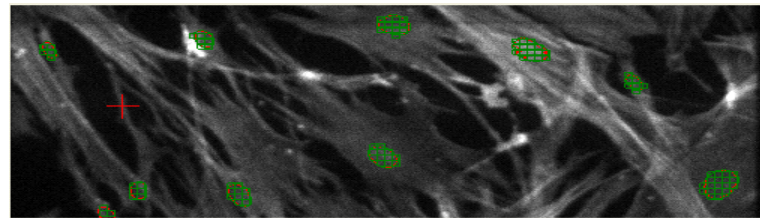
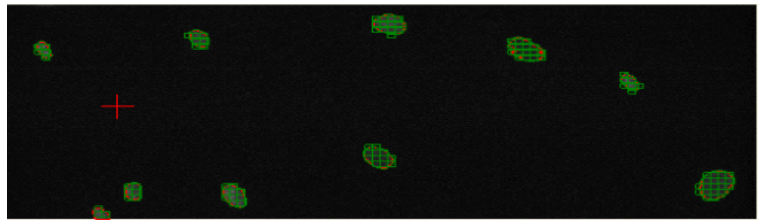
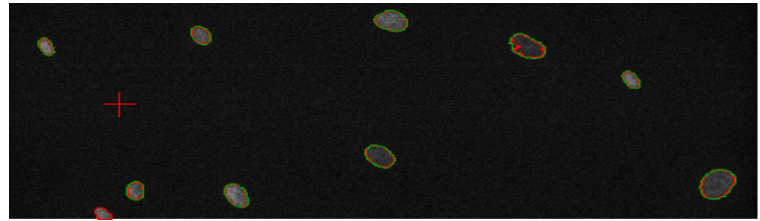


C

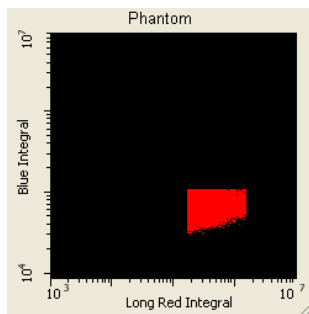
ROI selection of cell associated
- nuclear phantoms



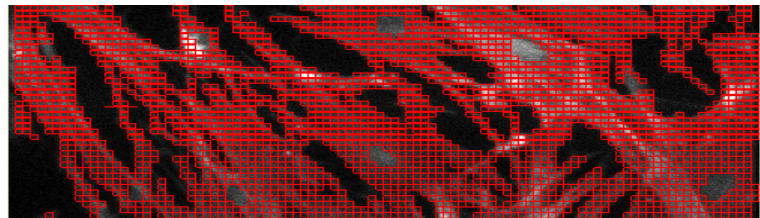
Map
ROI



Gate out both *background*
and *cell associated - nuclear*
phantoms.



Map
ROI



Cell associated - cytoplasmic phantoms are used for quantitation of G-Actin fluorescence

Cell Associated Cytoplasmic Phantoms

Figure 4.17. Isolation of nuclear associated phantoms. A) A scatter gram plot of blue (Hoechst) nuclear fluorescence versus long red (F-actin) cytoplasmic fluorescence reveals distinct phantom populations: Phantoms with low blue/low long red and low blue/high long red fluorescence (yellow box). Phantoms with low blue/high long red and high blue/high long red fluorescence (orange box). B) Cell associated phantoms previously identified in the phantom histogram, map to regions of low blue/high long red and high blue/high long red fluorescence within the phantom scatter gram. Phantoms with both high blue/high long red fluorescence (green box) are likely the cell associated- nuclear phantoms. ROI= region of interest.

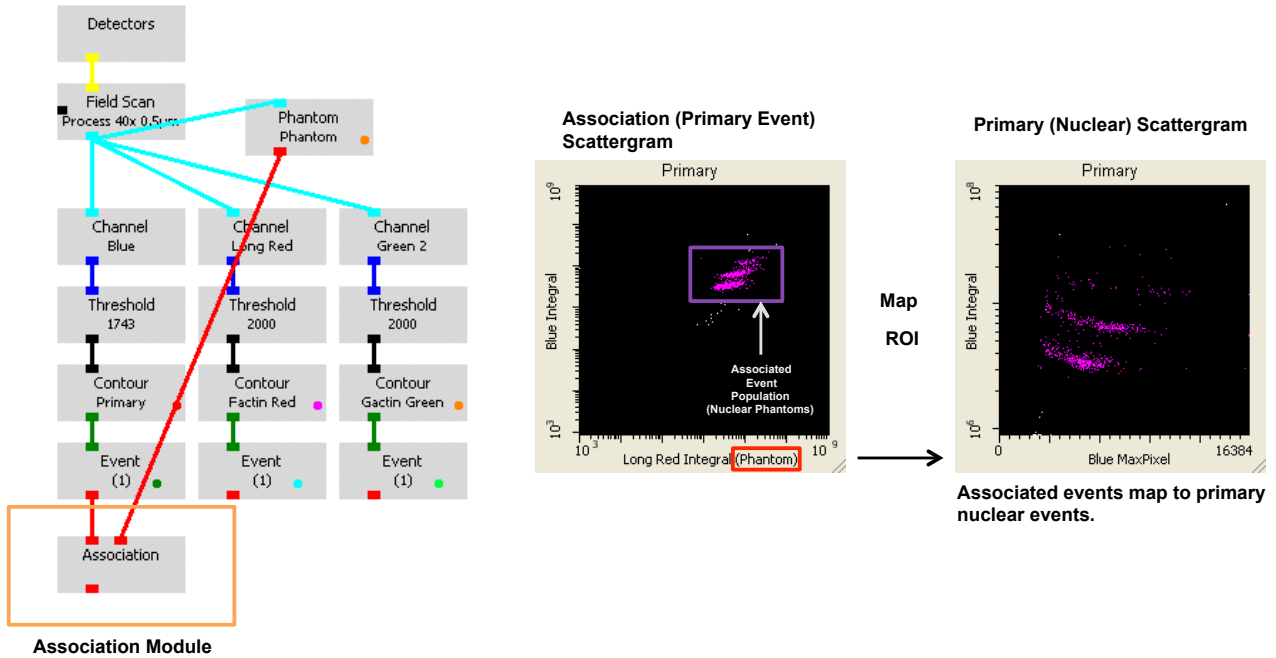
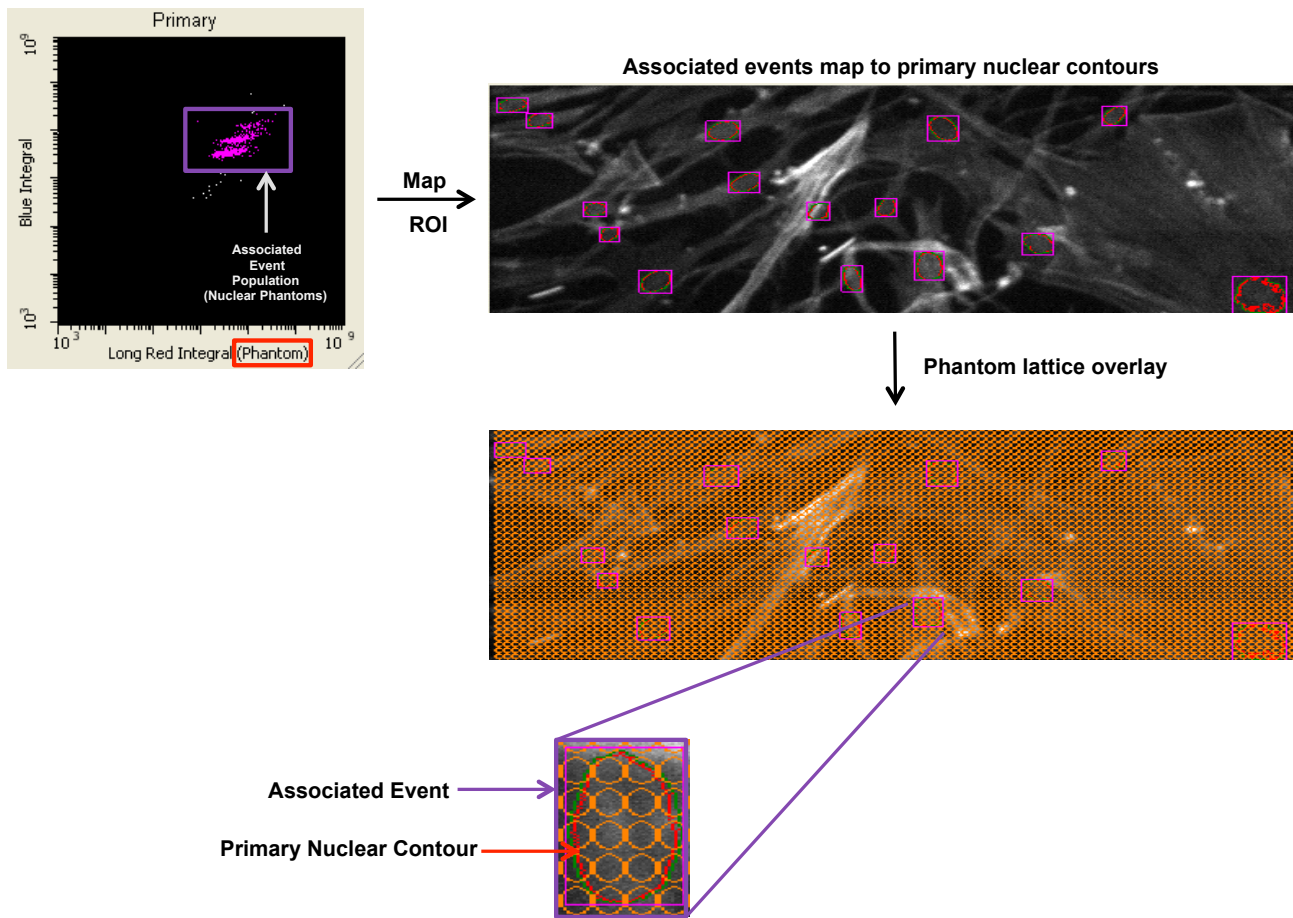
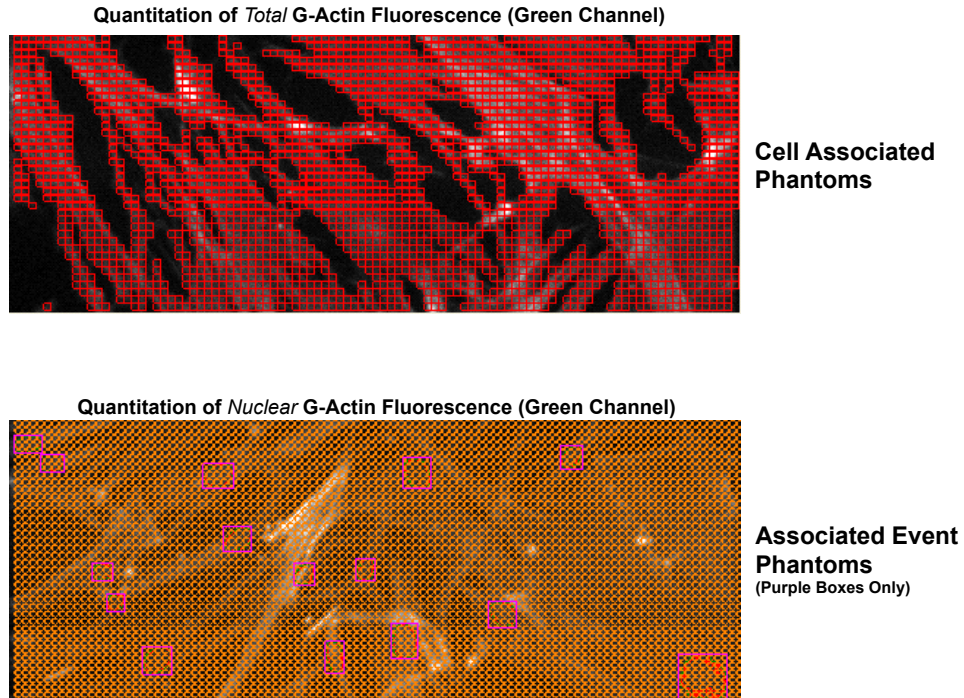


Figure 4.18. Nuclear associated phantom module. Phantoms links only phantom contours that are in direct contact with the primary contour (blue fluorescence) through the association module. The primary contour is the nucleolus phantom contour. The associated events are displayed using primary event scattergram and blotting nuclear (blue channel) fluorescence versus associated long red channel phantom fluorescence. This scattergram may be termed the association scattergram.

A



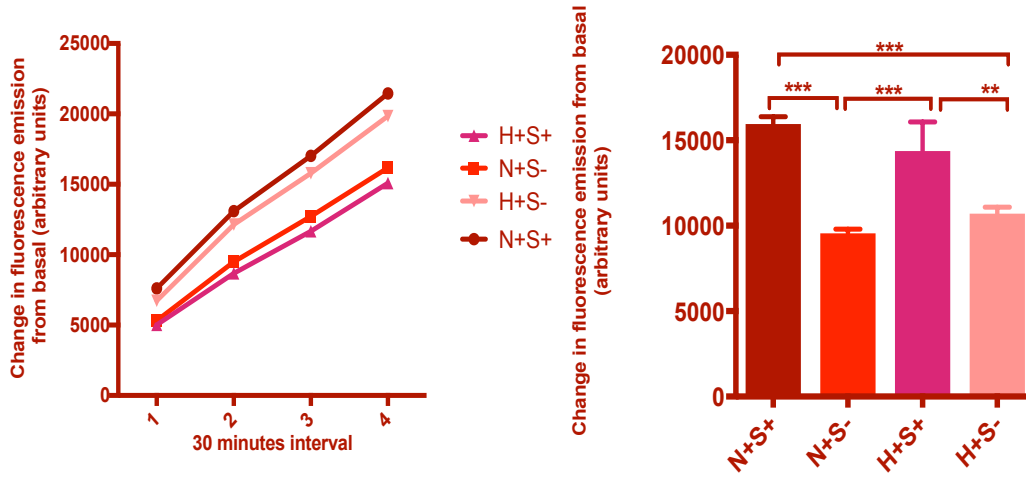
B



Total F-Actin		Total G-Actin		Nuclear G-Actin		Cytoplasmic G-Actin		
Phantom	Integral	Phantom	Integral	Phantom	Integral	Corrected Phantom		
Long Red Sum	Green Sum (Total)	(Nuclear)		Green	Sum	Integral Green	Sum	F:G-Actin Ratio (Sum)*
74,520,809,222	26,136,680,654	3,142,947,131				22,993,733,523		3.2

Figure 4.19. A) An alternative method of isolation of nuclear associated phantoms. B) The associated event population contains only those phantom contours in direct contact with the primary nuclear contour. C) *using this method, phantom population is consistent with the cell-associated nuclear phantom population isolated by the previous methodology.

A) Total ROS in PASM cells by DCF assay



B) Endogenous superoxide anion in PASM cells by DHE assay

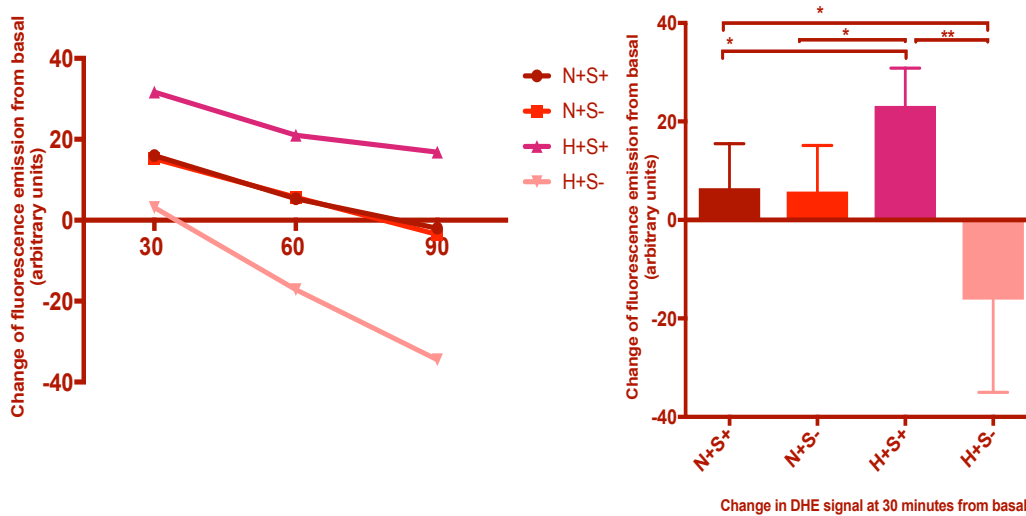


Figure 4.20. Pulsatile strain increased total ROS and superoxide release significantly in normoxic and hypoxic conditions. A) Total endogenous ROS is quantified by the change in DCF-DA fluorescence from primary PASM fibers. B) Endogenous superoxide radical is quantified by the change in DHE signal at 30 mins from basal induction. For both assays an average of 5×10^5 stimulated cells/treatment was analyzed during two consecutive 30 min periods at 37°C at excitation 485 nm, emission 520 nm and gain 1500. $P < 0.05$ represents significance, ***highly significant, Ratio to normoxic strain. N+S+=Normoxia together with stretch; N+S-= Normoxia independent on stretch; H+S+=Hypoxia together with stretch; H+S-=Hypoxia independent on stretch.

Appendix A

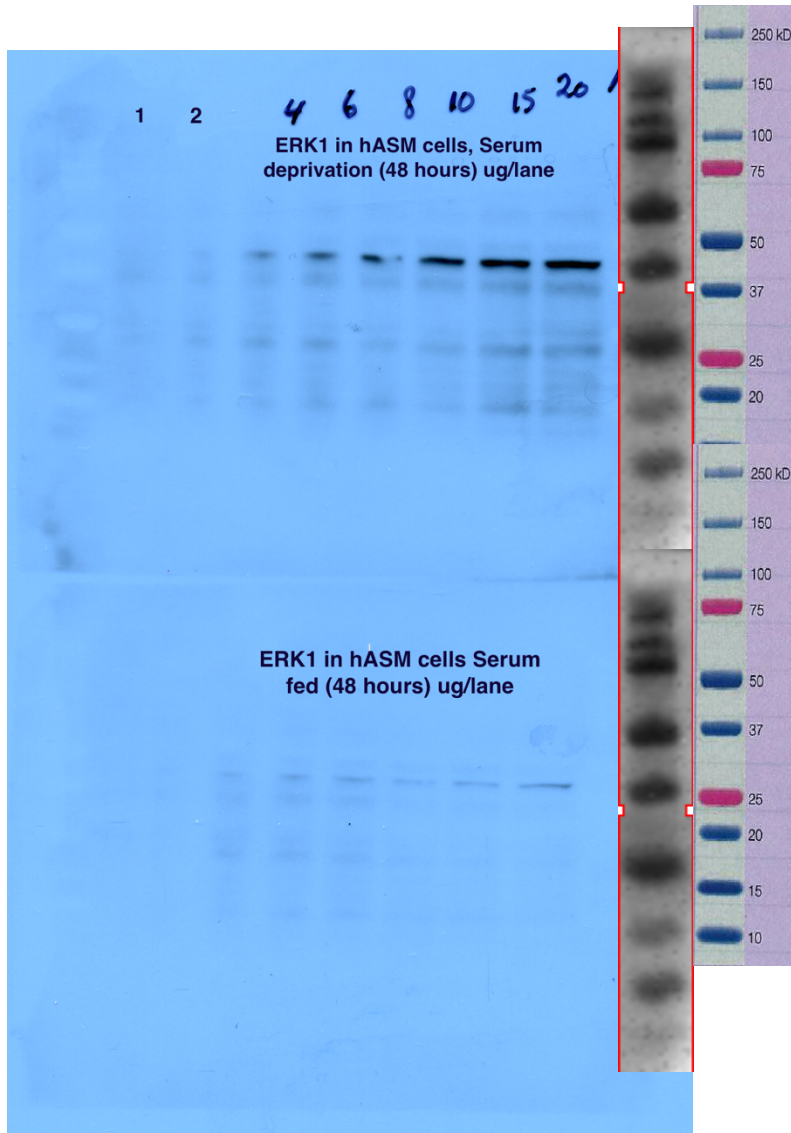


Figure A.1 Characterization of SM markers in hypertensive hASM cells. Concentration gradient shows the basal levels of ERK1 as it is expressed in serum fed and serum deprived hASM. Serum deprivation for 48 hours upregulated the basal expression ERK1. Full-length gel. Exposure: 2 mins. ERK 1=44 kDa.

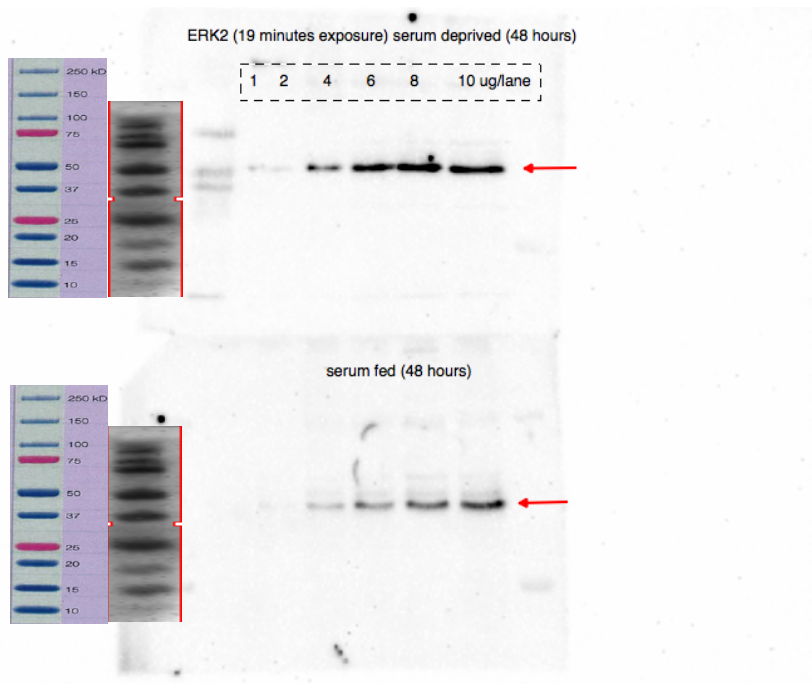


Figure A.2 Characterization of SM markers in hypertensive hASM cells. The concentration curve shows the basal levels of ERK2 as it is expressed in serum fed and serum deprived hASM. Serum deprivation for 48 hours upregulated the basal expression of ERK2. Full-length gel. Exposure: 2 mins. ERK2= 42 kDa.

2015-09-17 30 sec pERK1,2

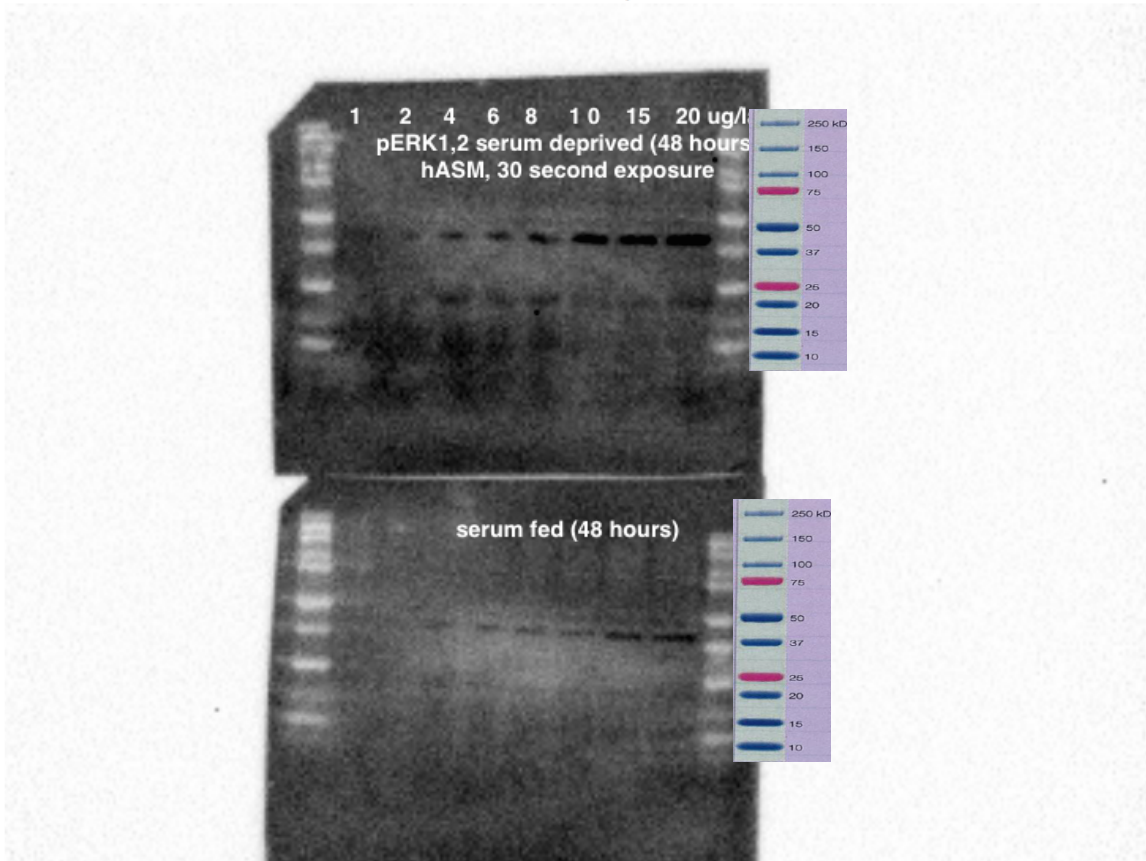


Figure A.3 Characterization of SM markers in hypertensive hASM cells. The concentration curve shows the basal levels of pERK1/2 as they are expressed in serum fed and serum deprived hASM. Serum deprivation for 48 hours upregulated the basal expression of pERK1/2. Full-length gel. Exposure: 30 sec. pERK1/2 appear on PAGE as two close bands of 44-42 kDa.

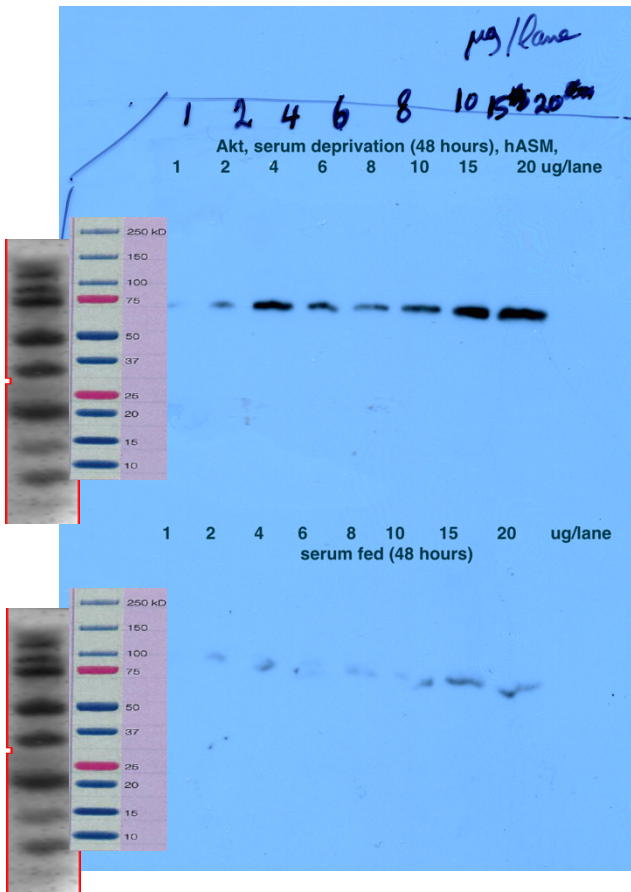


Figure A.4 Characterization of SM markers in hypertensive hASM cells. Concentration gradient shows the basal levels of AKT as it is expressed in serum fed and serum deprived hASM. Serum deprivation for 48 hours upregulated the basal expression of AKT. Full-length gel. Exposure: 4 mins. AKT=65 kDa.

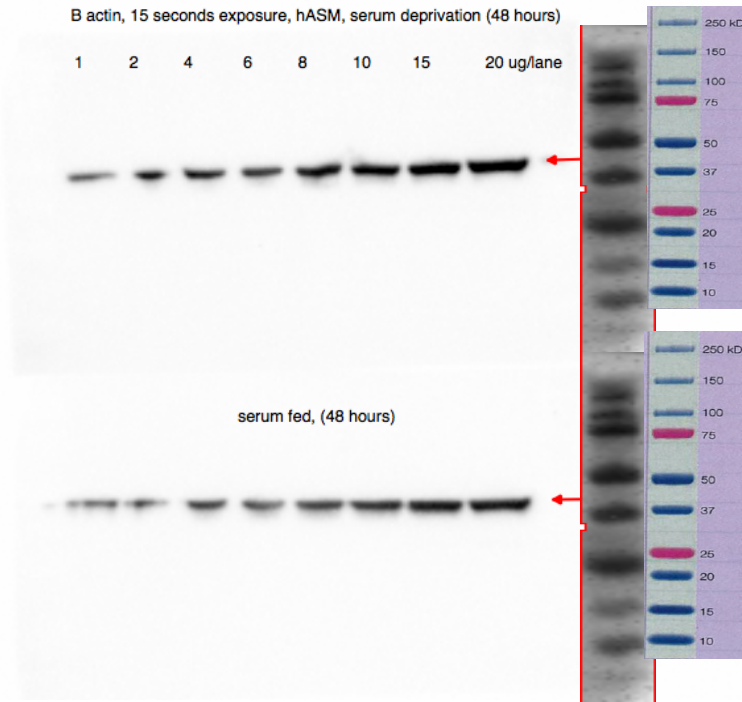


Figure A.5 Characterization of SM markers in hypertensive hASM cells. Concentration gradient shows the basal levels of β -actin as it is expressed in serum fed and serum deprived hASM. Serum deprivation for 48 hours upregulated the basal expression of β -actin. Full-length gel. Exposure: Exposure: 15 sec. β -actin= 42 kDa.

Desmin in PASM lysates (20 µg/lane)

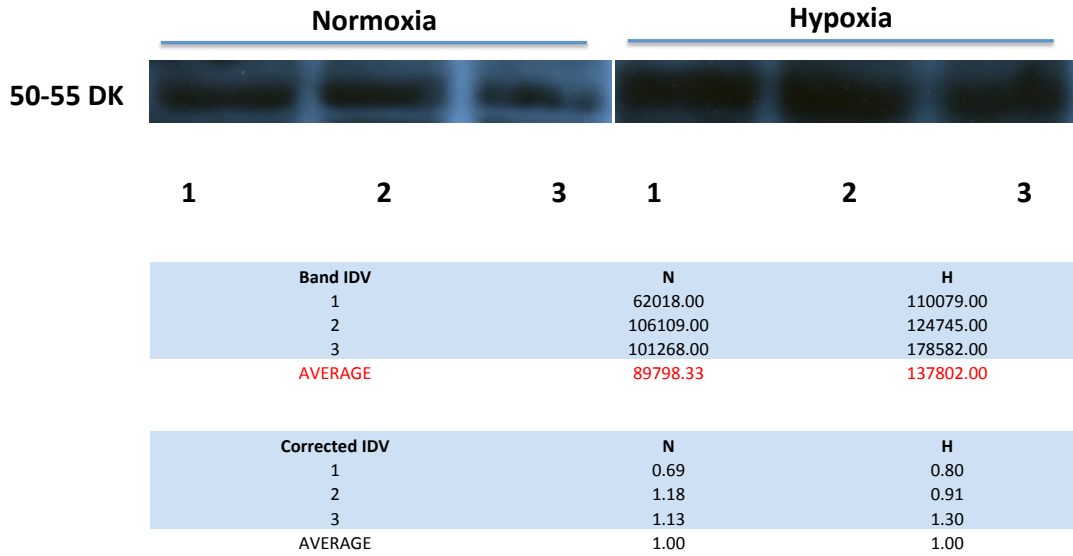


Figure A.6 Characterization of SM markers in hypertensive hASM cells. The data shows the basal levels of desmin as it is expressed in serum fed and serum deprived hASM. Serum deprivation for 48 hours upregulated the basal expression of desmin. Full-length gel. Exposure: Exposure: 15 sec.

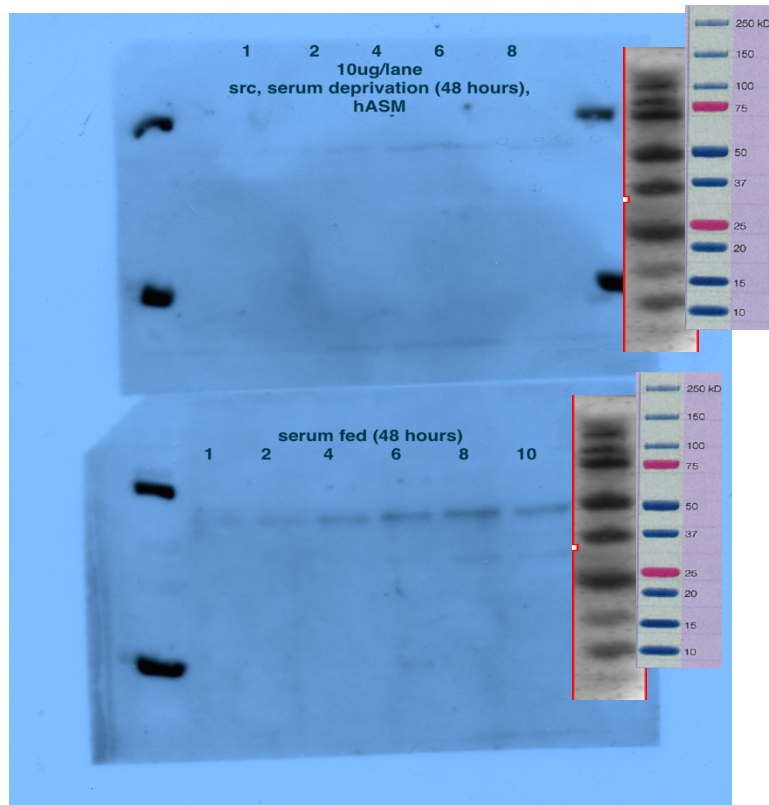


Figure A.7 Characterization of SM markers in hypertensive hASM cells. The data shows the basal levels of Src as it is expressed in serum fed and serum deprived hASM. Serum deprivation for 48 hours downregulated the basal expression of Src. Full-length gel. Exposure: Exposure: 15 sec. Src=55 kDa.

Appendix B

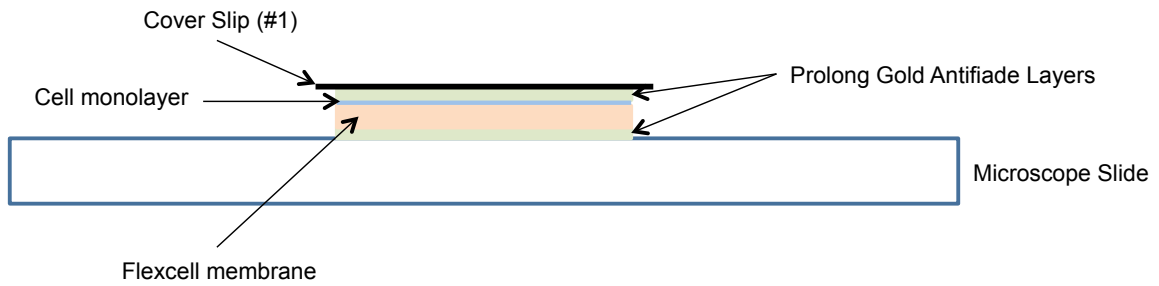


Figure B.1. Slide preparation. The membrane is affixed by mounting medium where cells side up.

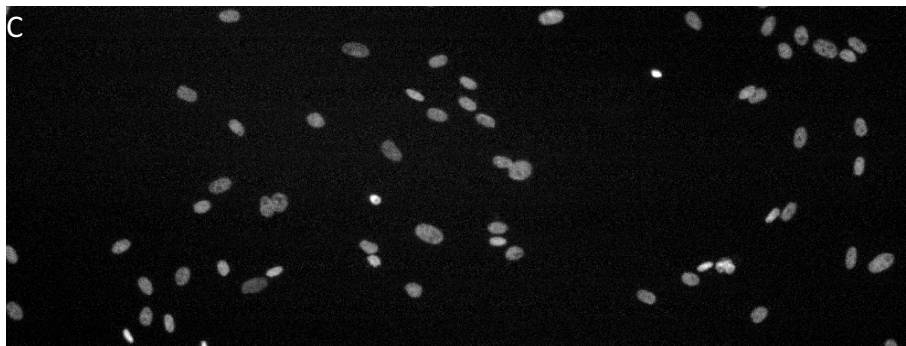
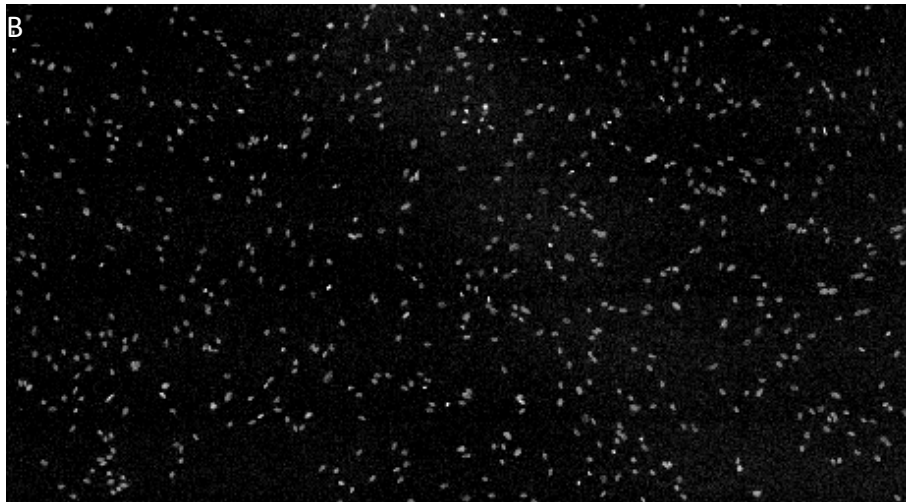
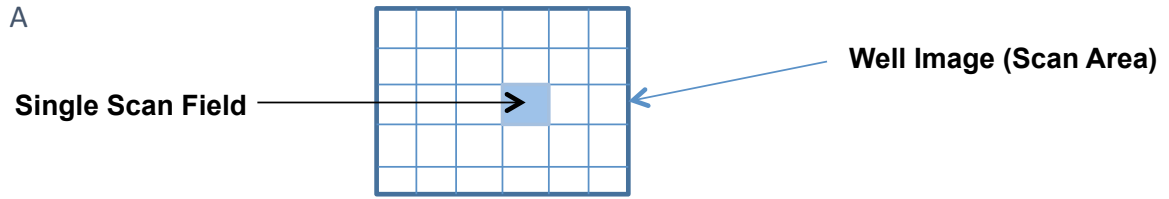


Figure B.2. Well image. A) Well image representative of the total area scanned with laser cytometer is a composite of single scan field images. B) a well image (scan area) of blue channels: Hoechst 33342 nuclear fluorescence from porcine PASM cells grown on flexer-cell plates. C) A larger view of a single scan field showing Hoechst nuclear fluorescence.

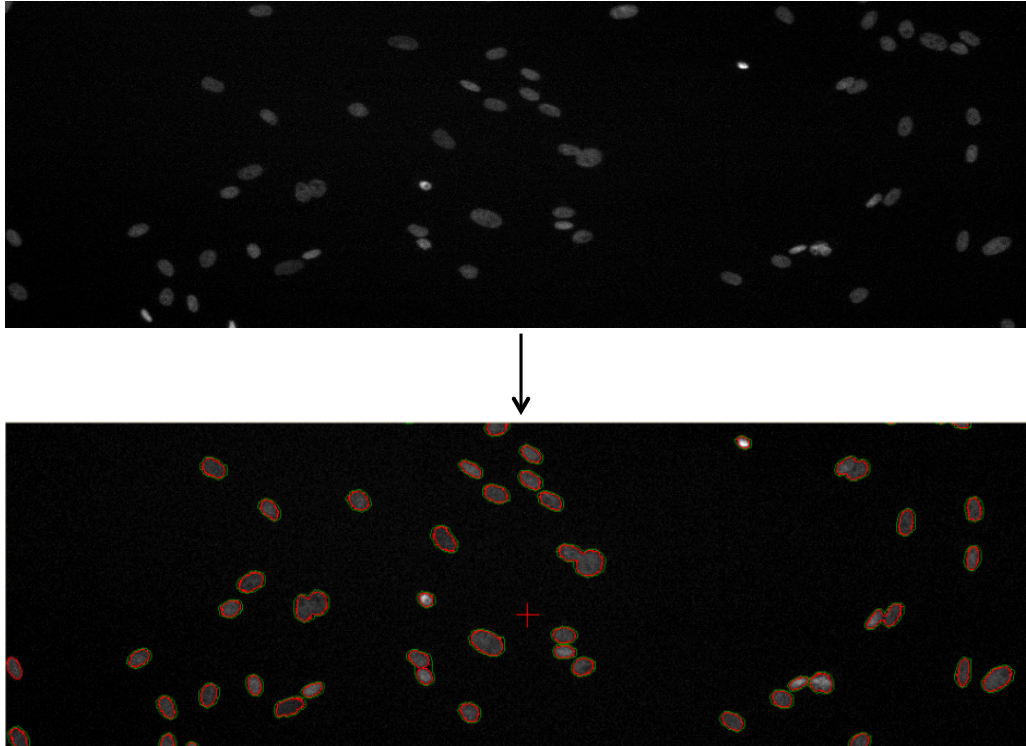


Figure B.3. Events before and after contouring. Blue channels: Hoechst 33342 nuclear fluorescence from porcine PASM cells grown on flexer-cell plates. How effectively I contour the threshold is controlled by the threshold module. Each one of the events is a separate quantitative measurement. The threshold contour (red) does not represent a boundary in which fluorescence is quantified. The true boundary for which fluorescence is quantified is defined by the integration contours (green). The reason is that sometimes the threshold contour does not outline the object all that effectively. The threshold is all or none. I cannot set contours for individual nuclei; I use a setting that is an average for all the events. The nucleolus has a brightness of three X. The other nucleolus is 0.5X in terms of brightness. The contour for the second nucleolus is not as precise, and lies inside the nucleus. Thus, some of the fluorescence is not included in the measurement. This can be corrected through the integration contour. The integration is drawn X pixels away from the threshold contour. To get the instrument to effectively contour the fluorescence and avoid getting noise, the threshold is set to a level at which the computer represents the fluorescent signal. The module image is a half-tone image of the field where the pixels are either black or white. By changing the scale, either white, black or in between, allows the software to judge which signals are noise and which are not. Setting the slider as a rough starting point is trying to reduce the noise to a minimum value without starting to lose the image of the nuclei. To judge what noise value is appropriate, right clicking on the image brings up the profile of the grey level value of the pixels. Placing the cursor on the threshold contour provides the value which can be used to distinguish between signal and noise. With this information, the integration contour can be set to a value sufficiently different from the threshold contour such that all the fluorescence will be collected. The integration contour represents the boundary in which the fluorescence is quantitated.

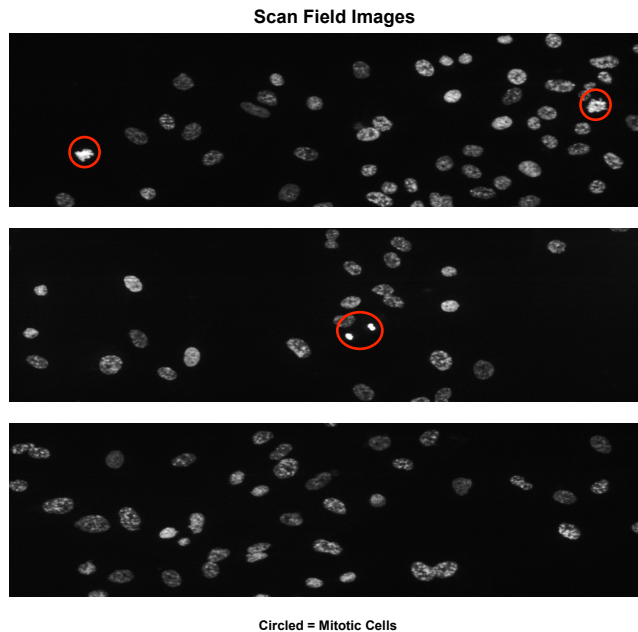


Figure B.4. Scan field images: mitotic events. Laser control voltage gain and offset will correspond to the image brightness. Mitotic nuclei are circled red. Nuclear fluorescence from porcine PASM cells grown on flexer-cell plates is obtained using Hoechst 33342 stain excited by the blue laser. Fluorescence is collected using PMT1. To get brighter fluorescence, the sensitivity of the detector is manipulated. The gain is always left in a 100. Additionally, I have to determine i) the field scan parameters, ii) the objective (25X for myocyte nuclei, 40X for cytosolic actin) and iii) the step size. It may also be necessary to modulate the offset, which is for the background fluorescence (how bright the background to the signal). Offset may be either a negative or a positive value. The PMT detector is a monochrome system that senses the grey level. Therefore, the computer is used to colour the image. This is just for visualization since it does not affect quantification; up to 5 colours can be selected.

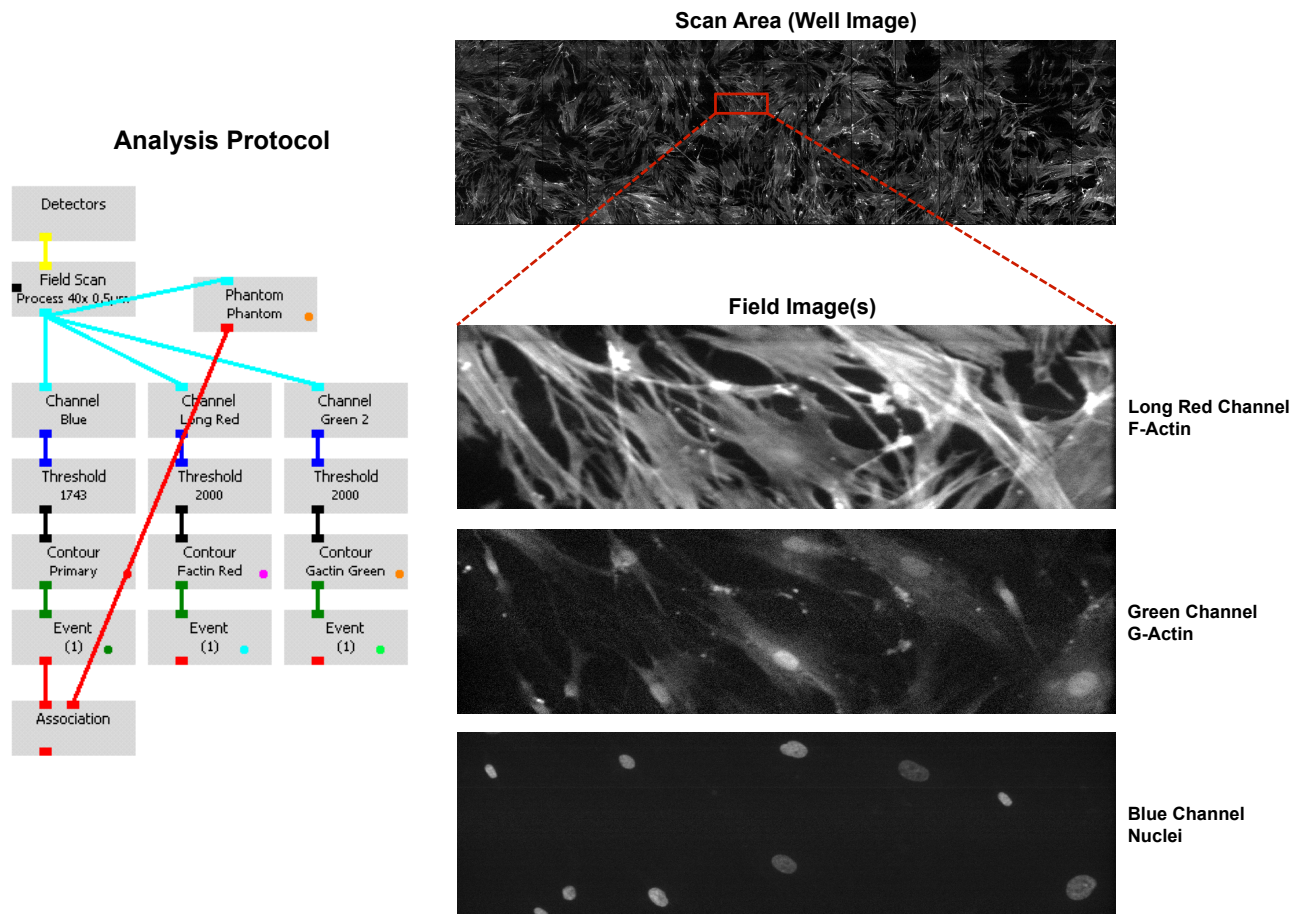


Figure B.5. Phantom contour analysis of cytoplasmic F:G-actin ratios in cultured hASM cells (HC82). Multiple channels are collected, with each assigned a separate colour. The F-actin contour is the red signal and the green is the G-actin. Phantom means a visual illusion that can define regions with distinctive boundaries when no real surrounding edges exist. Phantom contours are events generated by iCys from circular contours applied over the laser-scanned image. An Association module allows you to associate two event components generated with either an event module or a phantom module. There is primary and sub contour protocols. A one primary protocol is designed to analyze data using a single contour, and includes a phantom contour. The one primary, one sub protocol analyzes data using two contours. These are combined in the association module. The one primary, two sub contour protocol analyzes for a primary contour as well as two sub-contours, including an association among the three. It also provides a phantom contour module. I can break the connection with a module, but cannot connect the black module to a green module because they are colour coded, to make sure that they are in the right order, that are logistically related to one another by color code. Channel module cannot be connected to phantom because it is nonmeaningful. I can also disable a module down the chain event. If I want an association module I can click on and bring the association module and connect it with the primary event, which is the contour of the nucleus, and correlate it with phantoms.

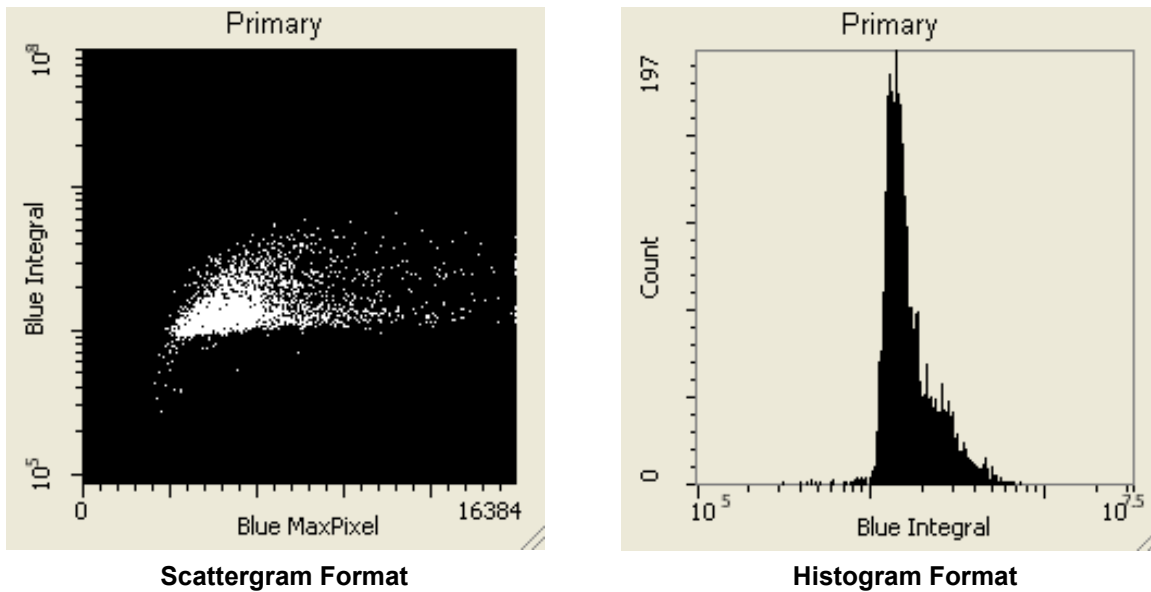
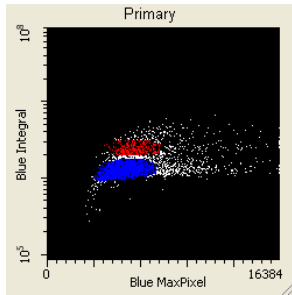
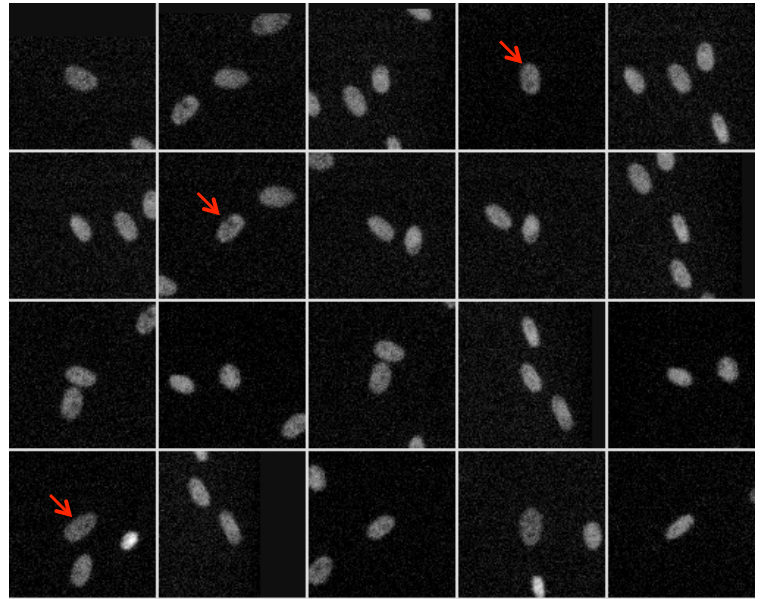


Figure B.6. Event data from Hoechst stained, non-treated normal nuclei of PASM grown in flex-plates. The event that I attempt to contour is called the primary event. In case of Hoechst, the nucleus is a primary event. The integrated fluorescence (intensity of the blue fluorescence) within each nucleus is placed on the Y axis. The X axis is the max pixel value of the blue fluorescence. The histogram provides the blue integration value (rather than an area, which is the default) on a log scale. Although it is possible to use a linear scale, the logarithmic scale is preferred if most of the data falls within a broad range. The integral blue = the total summed fluorescence (total summed grey level) within the boundary of the integration contour. The scattergram (X, Y position) creates a dot plot image of the scan area, with each dot representing an event (nucleus or actin fibers). Different populations can be colour coded blue, red or yellow to help identify which nuclei are associated with the population I interest in.

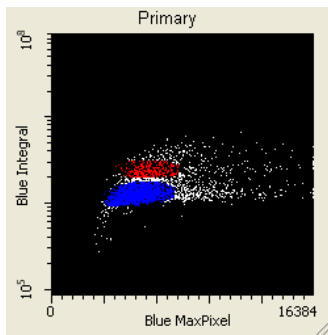
A



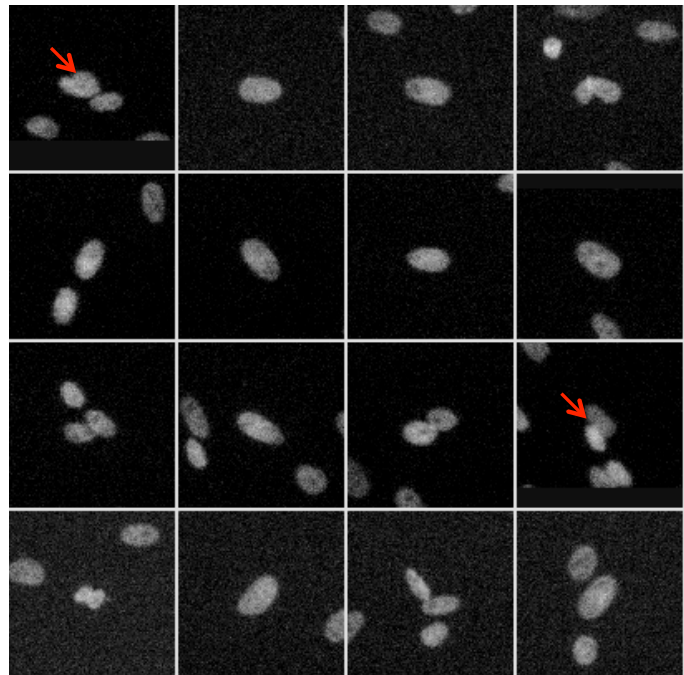
Gallery of Blue
Population: G0/G1
Nuclei



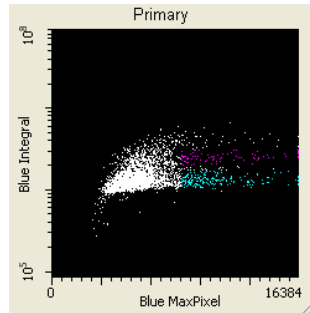
B



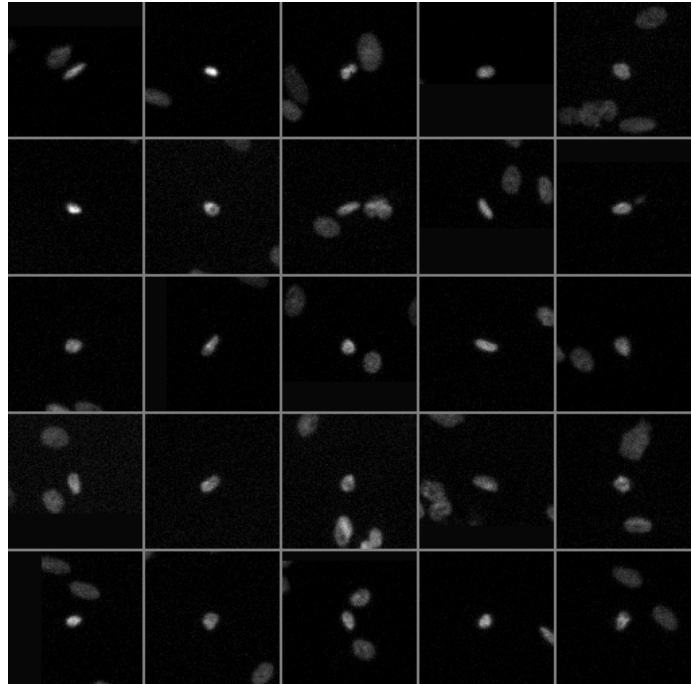
Gallery of Red
Population: G2
Nuclei



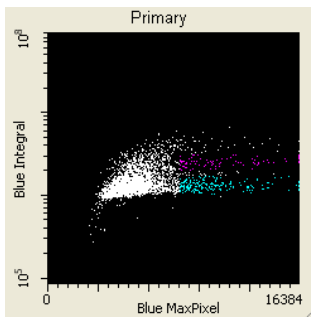
C



Gallery of Cyan
Population: Condensation
of G0/G1 nuclei



D



Gallery of Magenta
Population: Condensation
of G2 nuclei

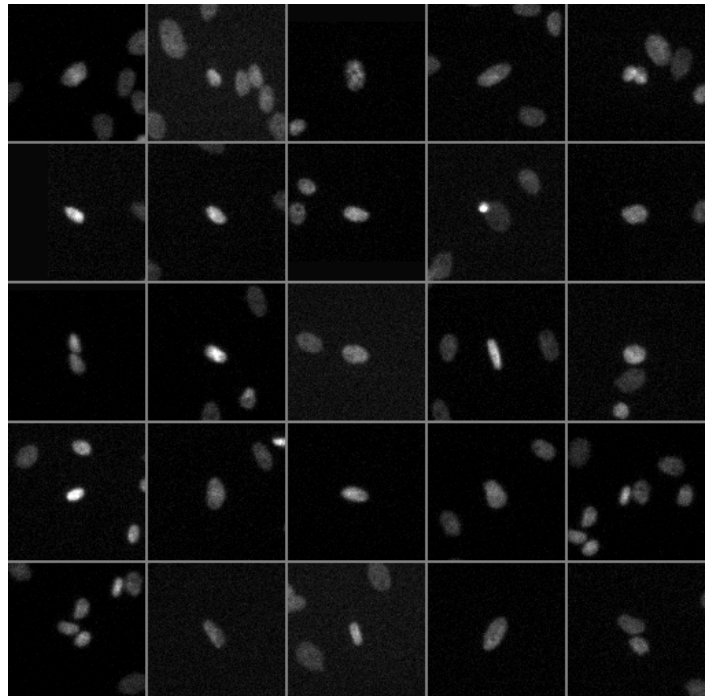


Figure B.7. Galleries. A) Gallery of cell cycle events in non-treated hASM cells (HC82). Multiple events may be found within any single gallery image. However, the event of interest is always that event located at the centre of the gallery image (arrows); B) Event population exhibits some contamination with contours of multiple nuclei. This is known as a problem with "segmentation" and results when fluorescent events are too closely spaced to be contoured effectively as single event arrows. C) hASM cells (HC82), no treatment. Gallery of cyan population: condensation of G0/G1 nuclei; D) gallery of magenta population: condensation of G2 nuclei.

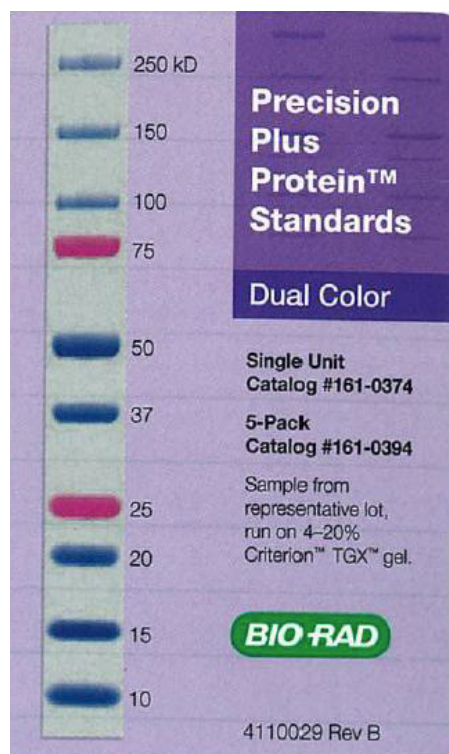
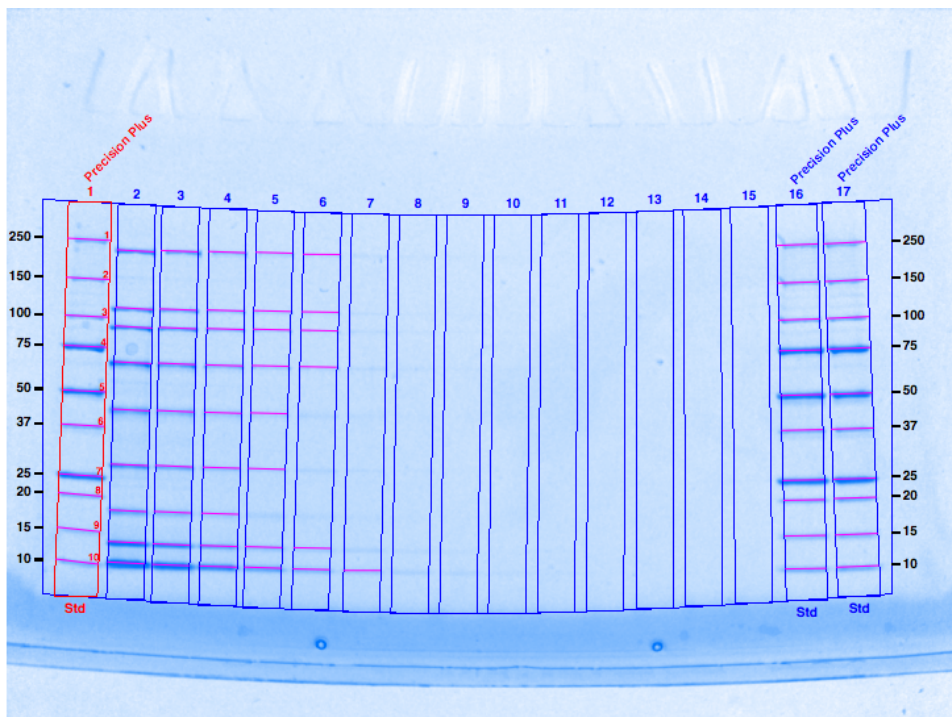


Figure B.8. Coomassie molecular ladder BioRad Precision Plus gel and specification.